ELSEVIER

Polymer 40 (1999) 6277–6296

polymer

Evolution of polymer blend morphology during compounding in an internal mixer

Je Kyun Lee, Chang Dae Han*

Department of Polymer Engineering, The University of Akron, Akron, OH 44325, USA

Received 4 November 1998; received in revised form 21 December 1998; accepted 28 December 1998

Abstract

The evolution of blend morphology during compounding in an internal mixer was investigated using transmission electron microscopy and scanning electron microscopy. Emphasis was placed on investigating the effects of viscosity ratio, blend composition, and processing variables (temperature, rotor speed, and mixing time) on the evolution of blend morphology in five blend systems: (i) nylon 6/high-density polyethylene (HDPE), (ii) poly(methyl methacrylate) (PMMA)/polystyrene (PS), (iii) polycarbonate (PC)/PS, (iv) PS/HDPE, and (v) PS/polypropylene (PP). These blend systems were chosen on the basis of the difference in the melting temperature (T_m) between two crystalline polymers (nylon 6/HDPE pair), the difference in the 'critical flow temperature' (T_{cf}) between two amorphous polymers (PMMA/PS and PC/PS pairs), or the difference between the T_{cf} of an amorphous polymer and the T_m of a crystalline polymer (PS/HDPE and PS/PP pairs). The T_{cf} of an amorphous polymer is de facto equivalent to the T_m of a crystalline polymer in that from a rheological point of view an amorphous polymer may be regarded as being a 'rubber-like solid' at temperatures below T_{cf} and a 'liquid' at temperatures above T_{cf}, which is approximately 55°C above the glass transition temperature (T_g) of an amorphous polymer. We observed a co-continuous morphology in PMMA/PS, PC/PS, PS/HDPE and PS/PP blends when the melt blend temperature was above the T_g, but below the T_{cf} of the constituent amorphous components, and a dispersed morphology when the melt blending temperature was increased far above the T_{cf} of the constituent amorphous components. Further, we found that the formation of a co-continuous morphology depends on blend composition and the viscosity ratio of the constituent components at a specified melt blending temperature. Most importantly, we have reached the conclusion that a co-continuous morphology is a transitory morphological structure that appears when a phase inversion takes place from one mode of dispersed morphology to another mode of dispersed morphology. The mode of a dispersed morphology is found to depend upon the blend composition and the viscosity ratio of the constituent components.

Keywords: Polymer blends; Co-continuous morphology; Dispersed morphology

1. Introduction

It has been a long-standing interest of polymer researchers in understanding the evolution of blend morphology when two (or more) incompatible homopolymers or copolymers are melt blended in a mixing equipment. In industry, melt blending is conducted using either an internal (batch) mixer (e.g. Banbury mixer; Brabender mixer) or a continuous mixer (e.g. twin-screw extruder; Buss Kneader).

When two immiscible polymers are compounded in a mixing equipment, two types of blend morphologies are often observed: dispersed morphology and co-continuous morphology. Numerous investigators reported on blend morphology of immiscible polymers and there are too many papers to cite all of them here. Some investigators [1–6] examined blend morphology to explain the seemingly very complicated rheological behavior of two-phase polymer blends, and others [7–14] investigated blend morphology as affected by processing conditions. However, in spite of much effort being spent on the subject, we still do *not* have a clear physical picture about the evolution of blend morphology during compounding in a mixing equipment. In the literature it is not clear as to under what conditions a dispersed morphology or a co-continuous morphology may be formed, and whether a co-continuous morphology is stable or it is an unstable intermediate morphology that eventually is transformed into a dispersed morphology.

The factors affecting the evolution of blend morphology during compounding are: (1) temperature, (2) duration of mixing in an internal mixer or the residence time in a twin-screw extruder, (3) the intensity of mixing (rotor speed in an internal mixer or screw speed in a twin-screw extruder), (4) blend composition, (5) viscosity ratio, (6) elasticity ratio, and (7) interfacial tension.

* Corresponding author. Tel.: + 1-330-972-6468; fax: + 1-330-972-5720.

0032-3861/99/$ - see front matter
PII: S0032-3861(99)00022-1

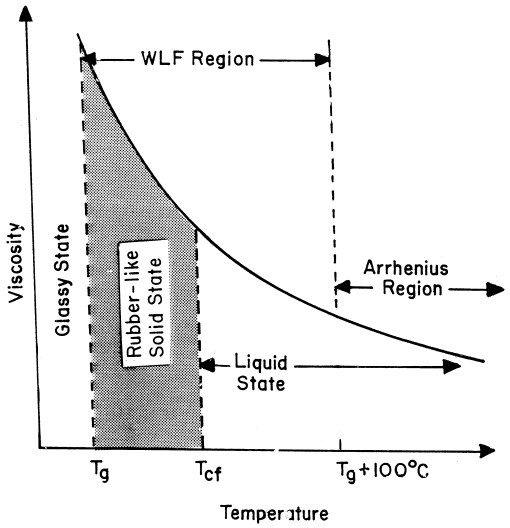

Fig. 1. Schematic describing the definition of critical flow temperature (T_{cf}) of an amorphous polymer [15].

Let us consider the morphology evolution in an immiscible blend consisting of two crystalline polymers, A and B, in a compounding machine and let us assume that the melting point ($T_{m,A}$) of polymer A is lower than the melting point ($T_{m,B}$) of polymer B. Under such circumstances, polymer A will melt first, forming the continuous phase in which the pellets (or powders) of polymer B will be suspended until the melt blending temperature reaches $T_{m,B}$, at which point the binary mixture will form an emulsion. As the temperature is increased further above $T_{m,B}$ (i.e. $T_{m,A} < T_{m,B} < T$), the evolution of blend morphology will depend on the viscosity ratio of the two polymers and blend composition. When the viscosity (η_A) of polymer A is lower than the viscosity (η_B) of polymer B and polymer A is the *major* component, most likely the blend will form a dispersed morphology having polymer A as the continuous phase and polymer B as the discrete phase (i.e. droplets). The droplets can be elongated and/or broken into smaller droplets, depending upon the intensity of the mixing and the viscosity ratio of the two polymers. An interesting question, however, can be raised. Would it be possible for polymer A to form the discrete phase and polymer B to form the continuous phase when polymer A is the *minor* component while maintaining the relationship $\eta_A < \eta_B$? The present study was motivated in part to answer the question posed before.

In order to understand the morphology evolution in an immiscible blend consisting of a crystalline polymer and an amorphous polymer in a mixing equipment, one must first define the temperature that can be regarded as being the *effective* 'melting point' of the amorphous polymer. From a thermodynamic point of view, an amorphous polymer can be regarded as 'liquid' at temperatures above its T_g. Practically, however, the viscosity of an amorphous polymer at temperatures slightly above T_g is so high, that the polymer hardly flows until reaching a certain temperature much higher than T_g, and thus the T_g of an amorphous polymer cannot be regarded as being a temperature that is *equivalent* to the melting temperature (T_m) of a crystalline polymer. Earlier, Shih [11] recognized the importance of this problem when melt blending a crystalline polymer (high-density polyethylene, HDPE) and an amorphous polymer (ethylene–propylene-terpolymer, EPDM). In his study, however, Shih did not elaborate on the temperature at which EPDM actually began to flow as 'liquid' during mixing with HDPE.

Previously, in a study on the plasticating extrusion of amorphous polymer in a single-screw extruder, Han et al. [15] introduced the concept of 'critical flow temperature' (T_{cf}), as schematically shown in Fig. 1, for amorphous polymers. With reference to Fig. 1, an amorphous polymer may be regarded as a 'rubber-like' solid at $T_g < T < T_{cf}$ and as a 'liquid' at $T \geq T_{cf}$, i.e. an amorphous polymer may be considered to *flow* at $T \geq T_{cf}$. In this regard, T_{cf} of an amorphous polymer is de facto equivalent to the 'melting point' of a crystalline polymer. Han et al. [15] found that for polystyrene and polycarbonate, $T_{cf} \approx T_g + 55$°C gave rise to a reasonably good agreement between measured pressure profiles along the extruder axis and model prediction.

Very recently, we carried out a systematic experimental investigation on the evolution of blend morphology, by scanning electron microscopy (SEM) and transmission electron microscopy (TEM), during melt blending of two immiscible homopolymers in an internal mixer. For the investigation, five pairs of polymers were selected: (i) two crystalline polymers, (ii) two pairs of polymers each consisting of two amorphous polymers, and (iii) two pairs of polymers each consisting of a crystalline polymer and an amorphous polymer. On the basis of the consideration presented earlier one can now easily surmise that when melt blending a crystalline polymer with an amorphous polymer, the difference between the T_m of the crystalline polymer and the T_{cf} of the amorphous polymer would play a very important role in determining the morphology evolution in such a blend. The present study thus was motivated in part by the desire to establish a firm scientific basis, on which one can predict morphology evolution in a polymer blend during compounding in terms of (i) the difference(s) in T_{cf} or T_m of the constituent components, (ii) blend composition, (iii) the viscosity ratio of the constituent components, (iv) mixing temperature, (v) rotor speed, and (vi) the duration of mixing. In this paper, we report the highlights of our findings.

2. Experimental

2.1. Materials

We employed six homopolymers: polystyrene (PS), poly(methyl methacrylate) (PMMA), polycarbonate (PC), high-density polyethylene (HDPE), polypropylene (PP), and nylon 6, as summarized in Table 1. Using these homopolymers we investigated the morphology evolution,

Table 1
Molecular characteristics of the polymers studied

Sample code	Manufacturer	Morphology	T_g or T_m (°C)
PMMA	Rohm and Haas (Plexiglas V825)	Amorphous	118
PS	Dow Chemical (STYRON 615PR)	Amorphous	98
PC	Dow Chemical	Amorphous	146
PP	Exxon Chemical (Escorene 1052)	Crystalline	165
HDPE	Dow Chemical (HF-1030 INSITE)	Crystalline	125
Nylon 6	AlliedSignal (Capron 8202)	Crystalline	221

during melt blending in a Brabender mixer, in each of the following five binary blend systems: (i) nylon 6/HDPE, (ii) PMMA/PS, (iii) PC/PS, (iv) PS/HDPE, and (v) PS/PP, as summarized in Table 2. Also given in Table 2 are (i) the value of ΔT_m between two crystalline polymers, nylon 6/HDPE blend, (ii) the values of ΔT_{cf} between two amorphous polymers, PMMA/PS and PC/PS blends, and (iii) the values of $|T_{cf} - T_m|$ between an amorphous polymer and a crystalline polymer, PS/HDPE and PS/PP blends. As will be shown later in this paper, the concept of T_{cf} is very important to interpret the morphology evolution in PMMA/PS, PC/PS, PS/HDPE, or PS/PP blends during melt blending in a Brabender mixer.

There are a very large number of polymer pairs that can be melt blended. However, we are of the opinion that the five polymer systems chosen in this study adequately represent many other conceivable polymer pairs from the point of view of the differences in T_m or T_g of the constituent crystalline and/or amorphous polymer components.

2.2. Rheological measurement

A Rheometrics Mechanical Spectrometer (Model RMS 800) with cone-and-plate fixture (25 mm diameter and 5° cone angle) was used, under a nitrogen atmosphere, to measure the shear viscosities of the six homopolymers (PS, PMMA, PC, HDPE, PP, and nylon 6) chosen over a very wide range of temperatures at low shear rates ranging from 0.001 to ca. 10 s^{-1}. An Instron capillary rheometer (Mode 3211, Instron Corporation) with a capillary diameter of 0.15 cm and a length-to-diameter ratio of 28.5 was used to measure the viscosities of the same homopolymers at high shear rates ranging from ca. 10 to 1000 s^{-1}.

Table 2
Polymer pairs employed for preparing blends

Sample code	Morphology	ΔT_{cf}, $\lvert T_{cf} - T_m \rvert$, or ΔT_m (°C)
PMMA/PS	Amorphous–amorphous	15[a,b]
PC/PS	Amorphous–amorphous	45[c]
PS/HDPE	Amorphous–crystalline	30[a]
PS/PP	Amorphous–crystalline	10[a]
Nylon 6/HDPE	Crystalline–crystalline	96

[a] T_{cf} of PS $\approx$ 155°C.
[b] T_{cf} of PMMA $\approx$ 170°C.
[c] T_{cf} of PC $\approx$ 200°C.

2.3. Mixing equipment and experimental procedures

Melt blending of a pair of polymers was conducted using an internal mixer (Brabender Plasticorder, Model FE-2000), which had two counter-rotating cam-type blades. In our experiment, two polymers at a given blend ratio were hand tumbled in a bag for about 30 min before being put into the mixing bowl, which had been heated to a preset temperature. In all experiments, about 70% of the total available volume was filled with material. Mixing time was counted from the time of sample loading into the mixing bowl, where about 15–30 s were required to load the sample. At different time intervals during compounding, a small amount of sample was taken from the mixer which took 3–5 s, and the sample was quenched in liquid nitrogen in order to freeze phase morphology and later kept in a refrigerator until microtoming. In preparing blends we varied blend composition, melt blending temperature, the intensity of mixing by varying the rotor speed of the Brabender Plasticorder, and the duration of melt blending.

2.4. Microscopy

A blend specimen was first embedded in an epoxy (EPON 828) and cured at room temperature using 10 wt.% triethylenetetramine; complete curing took about 24 h. The embedded samples were then ultramicrotomed using a Reichert Ultracut S (Leica) microtome equipped with glass knives. In order to have sufficient phase contrast in a melt-blended sample before using a microscope, the following methods were used, namely, PS was etched out selectively using toluene from PS/HDPE, PS/PP, and PC/PS blend samples and nylon 6 was etched out selectively using formic acid from a nylon 6/HDPE blend sample. Carbon black coating was applied to a PMMA/PS blend sample after ultramicrotoming. A transmission electron microscope (JEM 1200EX II, JEOL) operated at 100 kV was used to take micrographs of the PMMA/PS blend specimens. A scanning electron microscope (Hitachi, Model S-2150) was used to observe the phase morphology of PC/PS, PS/HDPE, PS/PP, and nylon 6/HDPE blend samples.

3. Results

3.1. Morphology evolution in blends consisting of two crystalline polymers

3.1.1. Nylon 6/HDPE blends

The upper panel of Fig. 2 gives the logarithmic plots of shear viscosity (η) versus shear rate ($\dot{\gamma}$) for nylon 6 and HDPE at 240°C, 250°C, and 260°C for $\dot{\gamma} =$ 0.001–1000 s^{-1}. The readers are reminded that values of

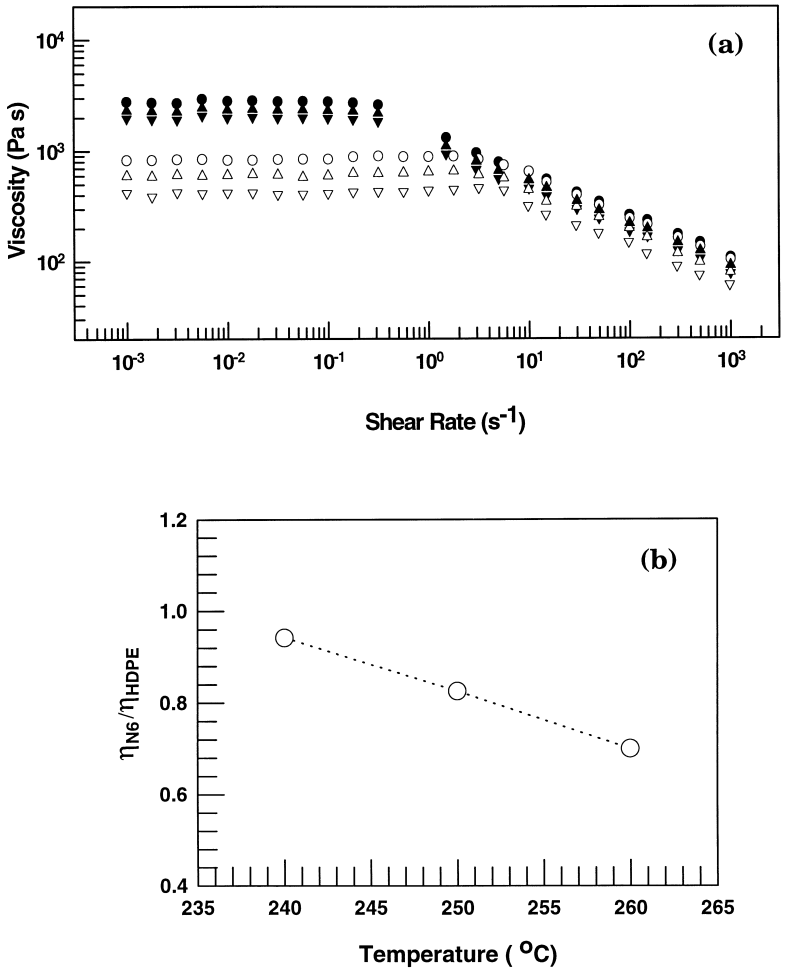

Fig. 2. (a) The upper panel describes the shear rate dependence of viscosity for nylon 6 (open symbols) and HDPE (filled symbols) at various temperatures: (○, ●) 240°C; (△, ▲) 250°C; (▽, ▼) 260°C. (b) The lower panel describes the temperature dependence of viscosity ratio, $\eta_{\text{nylon 6}}/\eta_{\text{HDPE}}$, at $\dot{\gamma} = 54.5\ \text{s}^{-1}$.

η at $\dot{\gamma} = 0.001$–$10\ \text{s}^{-1}$ were obtained using a cone-and-plate rheometer and values of η at $\dot{\gamma} = 10$–$1000\ \text{s}^{-1}$ were obtained using a capillary rheometer with a length-to-diameter ratio of 28.5 and thus without end corrections. The lower panel of Fig. 2 shows the dependence of viscosity ratio, $\eta_{\text{nylon 6}}/\eta_{\text{HDPE}}$, on temperature at $\dot{\gamma} = 54.5\ \text{s}^{-1}$, showing that $\eta_{\text{nylon 6}}/\eta_{\text{HDPE}}$ decreases with increasing temperature. It should be mentioned that $\dot{\gamma} = 54.5\ \text{s}^{-1}$ represents the maximum shear rate at a rotor speed of 50 rpm in the Brabender Plasticorder employed. Specifically, we estimated the shear rate in the Brabender Plasticorder using the expression $\dot{\gamma} = \Omega/\delta = \pi DN/\delta$, where Ω is the angular speed of the rotor tip, δ the gap opening between the rotor tip and the mixing chamber, D the diameter of the inner or outer rotor, and N the rotor speed in rpm. The outer diameter of the rotor was 37.5 mm with $\delta = 1.8$ mm, and the inner diameter of the rotor was 12 mm with $\delta = 27.3$ mm. Thus we took the maximum value of $\dot{\gamma} = 54.5\ \text{s}^{-1}$, estimated from the expression given above, to approximately represent the intensity of mixing in the Brabender Plasticorder at a rotor speed of 50 rpm. We are well aware of the fact that the simplistic approach adopted here is not rigorous, but we have done this only to relate the intensity of mixing to shear rate, thus enabling us to estimate the viscosity ratio of the constituent components. Throughout this paper, we put emphasis on the viscosity ratio of the constituent components to interpret the morphology evolution observed during compounding in a Brabender Plasticorder.

Fig. 3 shows the SEM images of the 30/70, 50/50, and 70/30 nylon 6/HDPE blends, which were prepared at 240°C at a rotor speed of 50 rpm for 2, 5, and 10 min, where the dark areas represent the nylon 6 phase and the light areas represent the HDPE phase. Note that since T_m of nylon 6 is 221°C and T_m of HDPE is 125°C, the HDPE melts first, forming the matrix phase in which nylon 6 pellets are suspended until the temperature reaches 221°C. Upon melting at 221°C, the nylon 6 becomes droplets and then two possibilities exist: either nylon 6 droplets remain as the discrete phase and are dispersed in the HDPE matrix or the discrete phase of nylon 6 transforms into the continuous phase, thus phase inversion takes place.

In Fig. 3(a)–(c) we observe that (i) after 2 min of mixing the 30/70 nylon 6/HDPE blend already formed a well-established dispersed morphology, in which the nylon 6 forms

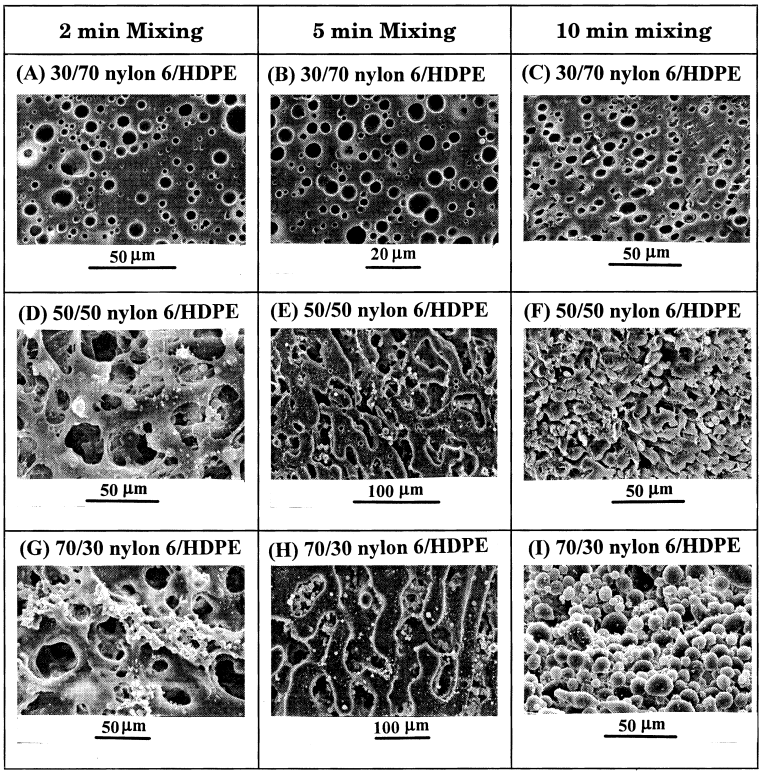

Fig. 3. SEM images describing the effect of mixing time (2, 5, or 10 min) on the morphology evolution in the 30/70, 50/50, and 70/30 nylon 6/HDPE blends during compounding at a rotor speed of 50 rpm and at 240°C in a Brabender Plasticorder.

droplets and is dispersed in the HDPE matrix; and (ii) the same morphology persisted when the mixing time was extended to 10 min. The readers are reminded that the HDPE has a higher viscosity than the nylon 6 (see Fig. 2). Thus we are led to conclude that blend ratio determined the state of dispersion in the 30/70 nylon 6/HDPE blend.

If blend ratio were to determine the mode of dispersion in the 70/30 nylon 6/HDPE blend, we expect that the major component nylon 6 would form the continuous phase and the minor component HDPE would form the discrete phase. This means that phase inversion must take place after a sufficiently long mixing time, because the HDPE melts first form the continuous phase while the nylon 6 stays as solid pellets until the melt blending temperature reaches the T_m (221°C) of nylon 6. Indeed the SEM micrographs of the 70/30 nylon 6/HDPE blend demonstrates this being the case, as can be seen in Fig. 3(g)–(i). Specifically, during the initial 2 min of mixing, nylon 6 formed the discrete phase (dark holes in Fig. 3(g)) and the HDPE formed the continuous phase. As the mixing continued for 5 min, we observed a co-continuous morphology consisting of interconnected structures of nylon 6 and HDPE (Fig. 3(h)). As the mixing continued for 10 min, we observed a dispersed morphology in which HDPE is dispersed in the continuous nylon 6 phase (Fig. 3(i)).

In Fig. 3(d)–(f) we observe a morphology evolution in the 50/50 nylon 6/HDPE blend, which is very similar to that in the 70/30 nylon 6/HDPE blend discussed earlier (Fig. 3(g)–(i)). The blend composition being symmetric in the 50/50 nylon 6/HDPE blend, we conclude that the viscosity ratio determined the state of dispersion in that the more viscous HDPE formed the discrete phase and the less viscous nylon 6 formed the continuous phase.

What is of great interest in Fig. 3 is that a co-continuous morphology is a transitory morphological state, through which one mode of dispersed morphology is transformed into an another mode of dispersed morphology. In other words, we tentatively conclude that the co-continuous morphology observed in the 50/50 and 70/30 nylon 6/HDPE blends is not stable. If we did not continue melt blending experiment for a sufficiently long period (say 10 min), we might have erroneously concluded that the 50/50 and 70/30 nylon 6/HDPE blends have a co-continuous morphology. This observation suggests that melt blending be continued for a sufficiently long period in order to observe a stable phase morphology in immiscible polymer blends.

3.2. Morphology evolution in blends consisting of two amorphous polymers

3.2.1. PMMA/PS blends

The upper panel of Fig. 4 gives log η versus log $\dot{\gamma}$ plots for PMMA and PS at 160°C, 170°C, 180°C, 200°C, 220°C, and 240°C for $\dot{\gamma} = 0.001$–$1000\ s^{-1}$. It can be seen that the viscosity of PMMA is much greater than that of PS over the

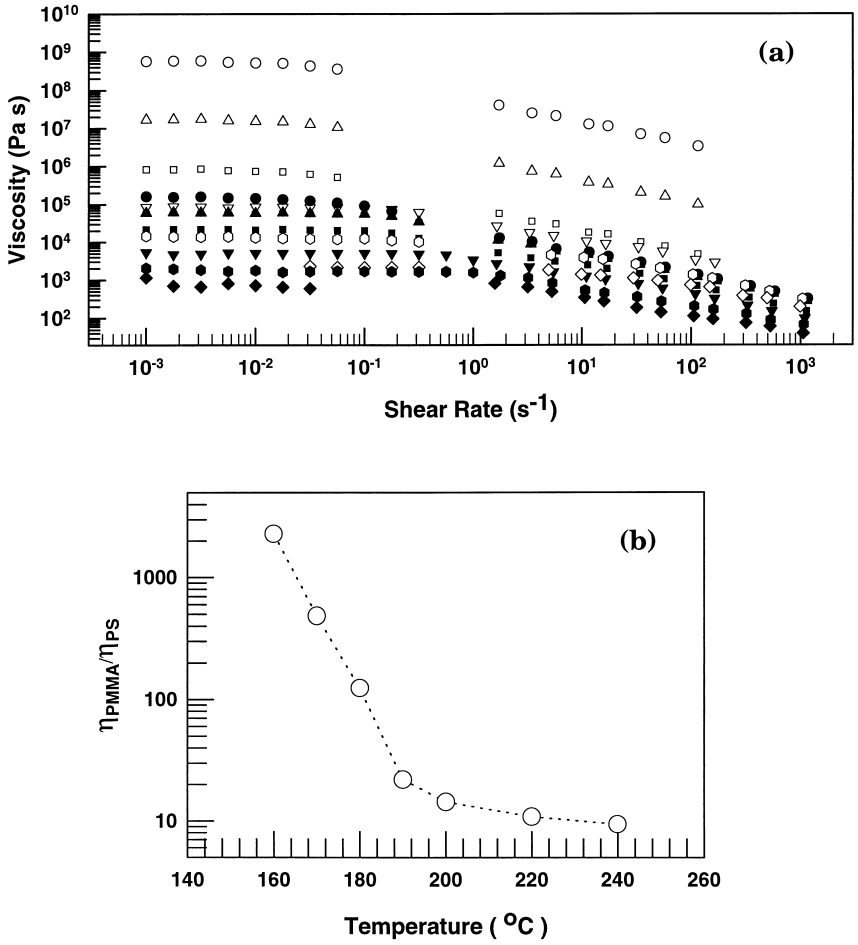

Fig. 4. (a) The upper panel describes the shear rate dependence of viscosity for PMMA (open symbols) and PS (filled symbols) at various temperatures: (○, ●) 160°C; (△, ▲) 170°C; (□, ■) 180°C; (▽, ▼) 200°C; (○, ●) 220°C; (◇, ◆) 240°C. (b) The lower panel describes the temperature dependence of viscosity ratio, η_{PMMA}/η_{PS}, at $\dot{\gamma} = 54.5\ s^{-1}$.

entire range of temperatures and shear rates tested, especially at low $\dot{\gamma}$. In order to facilitate our discussion later, the dependence of viscosity ratio, η_{PMMA}/η_{PS}, on temperature at $\dot{\gamma} = 54.5\ s^{-1}$ is presented in the lower panel of Fig. 4. It can be seen that the η_{PMMA}/η_{PS} ratio is very high at 160°C, decreases rapidly as the temperature increases from 160°C to ca. 190°C, and then tends to level off at 220°C and higher.

Fig. 5 gives the TEM images of the 70/30, 50/50, and 30/70 PMMA/PS blends, which were prepared at a rotor speed of 50 rpm at 160°C for 5 and 30 min of mixing, where the dark areas represent the PS phase and the white areas represent the PMMA phase. It is of interest to observe in Fig. 5 a co-continuous morphology in all three blend compositions, regardless of whether they were mixed for 5 or 30 min. The melt blending temperature employed, 160°C, was close to the T_{cf} (155°C) of PS and below the T_{cf} (170°C) of PMMA. This observation suggests that during melt blending at 160°C the PS barely functioned as a 'liquid' and the PMMA functioned as a 'rubber-like solid' (see Fig. 1). Notice from Fig. 4 that at 160°C, $\eta_{PMMA}/\eta_{PS} \approx 2200$ at $\dot{\gamma} = 54.5\ s^{-1}$, indicating that there hardly could have been any meaningful mixing between PMMA and PS at 160°C. This consideration can now explain why in Fig. 5 a co-continuous morphology is observed in all three blend compositions, regardless of whether each blend was mixed for 5 or 30 min.

Fig. 6 gives the TEM images of the 70/30, 60/40, 55/45, 50/50, and 30/70 PMMA/PS blends, which were prepared at a rotor speed of 50 rpm at 200°C for 5 and 30 min of mixing. Note that the melt blending temperature employed, 200°C, is higher than the T_{cf}s of both PMMA and PS, and that at 200°C $\eta_{PMMA}/\eta_{PS} \approx 12$ at $\dot{\gamma} = 54.5\ s^{-1}$ (see Fig. 4). The following observations are worth noting in Fig. 6. For 5 min mixing, the 70/30 PMMA/PS blend has a well-developed dispersed morphology in which PS forms the discrete phase and PMMA forms the continuous phase. In contrast, for the same duration of mixing, the 30/70 PMMA/PS blend has a well-developed dispersed morphology in which PMMA forms the discrete phase and PS forms the continuous phase. As mixing was extended to 30 min, the morphology of both the 70/30 and 30/70 PMMA/PS blends remained more or less the same. From the above observation we tentatively conclude that in the 70/30 and 30/70 PMMA/PS blends the major component forms the continuos phase

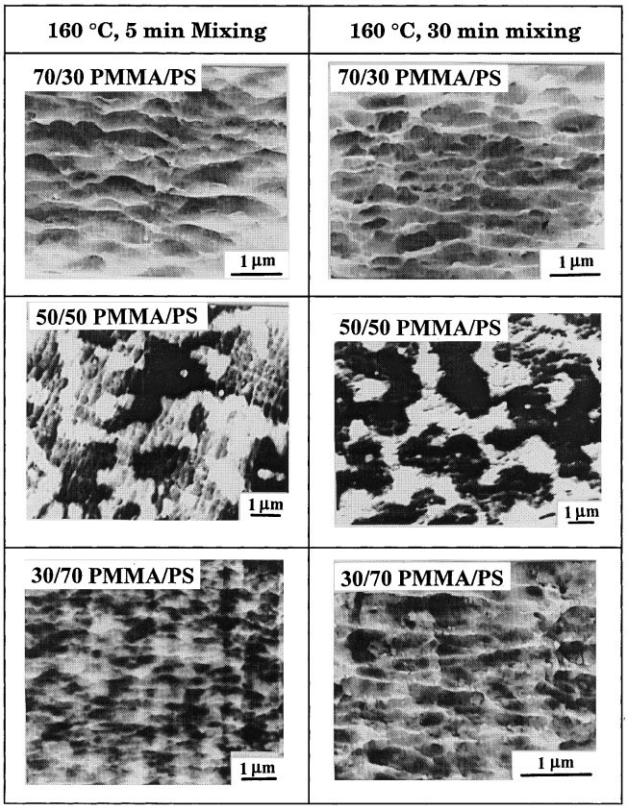

Fig. 5. TEM images describing the effect of mixing time (5 versus 30 min) on the morphology evolution in the 70/30, 50/50, and 30/70 PMMA/PS blends during compounding at a rotor speed of 50 rpm and at 160°C in a Brabender Plasticorder.

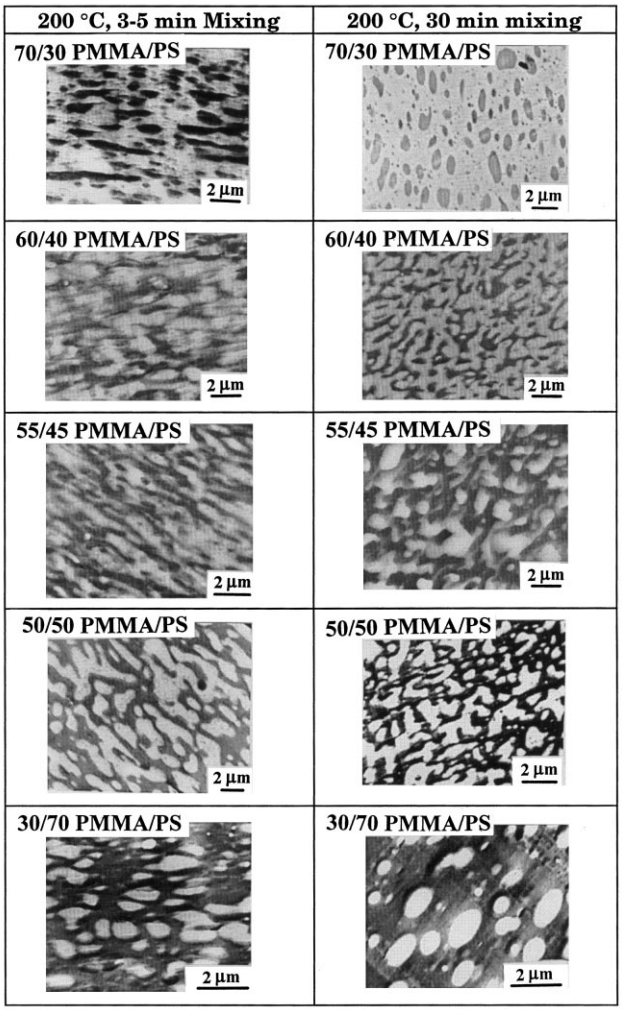

Fig. 6. TEM images describing the effect of mixing time (5 versus 30 min) on the morphology evolution in the 70/30, 60/40, 55/45, 50/50, and 30/70 PMMA/PS blends during compounding at a rotor speed of 50 rpm and at 200°C in a Brabender Plasticorder.

and the minor component forms the discrete phase, i.e. blend ratio determines the state of dispersion regardless of the viscosity ratio of the constituent components. Interestingly, we observe that in the 50/50 PMMA/PS blend the more viscous PMMA forms the discrete phase and the less viscous PS forms the continuous phase, suggesting that the viscosity ratio of the constituent components determines the state of dispersion for an equal blend composition. However, we observe a co-continuous morphology in the 60/40 PMMA/PS blend even after melt blending for 30 min at 200°C. In order to ascertain whether or not the co-continuous morphology observed in the 60/40 PMMA/PS blend could be regarded as being stable, we conducted further experiments by increasing melt blending temperature from 200°C to 220°C and to 240°C, and by increasing the rotor speed from 50 to 150 rpm.

In Fig. 7 we observe that increasing melt blending temperature from 200°C to 220°C and increasing rotor speed from 50 to 150 rpm produced a well-developed dispersed morphology in the 60/40 PMMA/PS blend, in which the minor component PS forms the discrete phase and the major component PMMA forms the continuous phase, in spite of the fact that PMMA is more viscous than PS. Also, increasing melt blending temperature from 220°C to 240°C at a rotor speed of 50 rpm produced a well-developed dispersed morphology in the 60/40 PMMA/PS blend, in which the minor component PS forms the discrete phase and the major component PMMA forms the continuous phase. From the above observations we tentatively conclude that the co-continuous morphology observed in the PMMA/PS blend is not stable, but a transitory morphological state before the blend transforms into a dispersed morphology that can be achieved either by increasing melt blending temperature or by increasing the rotor speed (i.e. by increasing the intensity of mixing).

3.2.2. PC/PS blends

The upper panel of Fig. 8 gives the log η versus log $\dot{\gamma}$ plots for PC and PS at 200°C, 220°C, and 240°C for $\dot{\gamma} = 0.001$–$1000\ s^{-1}$, showing that the viscosity of PC is higher than that of PS at all temperatures and $\dot{\gamma}$ investigated. Notice in Fig. 8 that PC has a very weak shear-thinning behavior even at very high $\dot{\gamma}$, while PS exhibits considerable

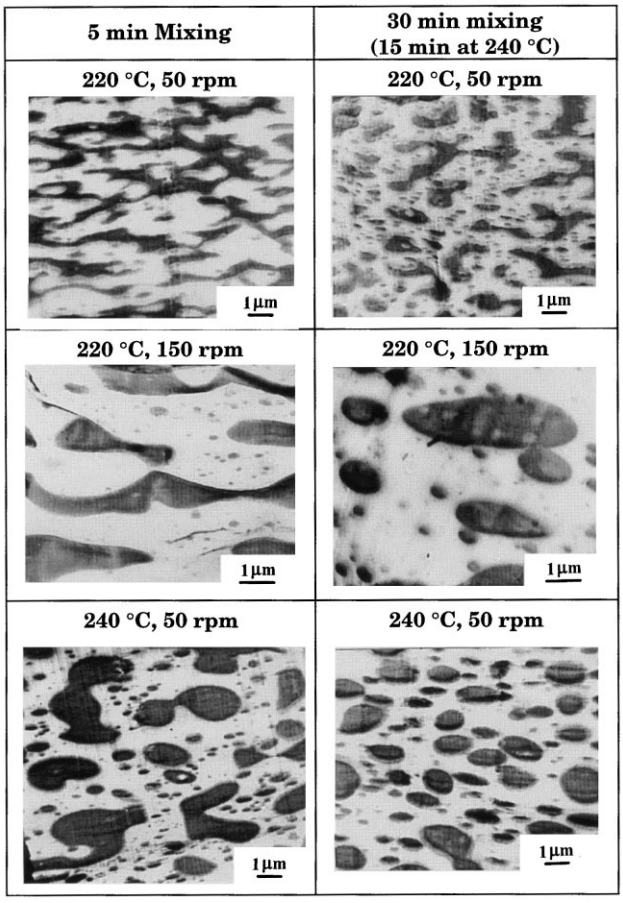

Fig. 7. TEM images describing the effect of mixing time (3–5 versus 30 min), rotor speed (50 versus 150 rpm), and melt blending temperature (220°C versus 240°C) on the morphology evolution in the 60/40 PMMA/PS blend during compounding in a Brabender Plasticorder.

shear-thinning behavior. In order to facilitate our discussion later, the dependence of viscosity ratio, η_{PC}/η_{PS}, on temperature is presented in the lower panel of Fig. 8 at $\dot{\gamma} = 10.9\ s^{-1}$ (corresponding to a rotor speed of 10 rpm), $54.5\ s^{-1}$ (corresponding to a rotor speed of 50 rpm), $109\ s^{-1}$ (corresponding to a rotor speed of 100 rpm), and $163.5\ s^{-1}$ (corresponding to a rotor speed of 150 rpm). This information will be useful to interpret morphology evolution in the PC/PS blends later. It can be seen that the η_{PC}/η_{PS} ratio is very large at high $\dot{\gamma}$ compared to that at low $\dot{\gamma}$, which is attributable to the fact that the PC exhibits a very weak shear-thinning behavior while PS exhibits a strong shear-thinning behavior at high $\dot{\gamma}$. Note further that the η_{PC}/η_{PS} ratio is very large at 200°C and 220°C for $\dot{\gamma} = 54.5\ s^{-1}$ and higher.

Fig. 9 gives the SEM images of the 70/30, 50/50, and 30/70 PC/PS blends, which were prepared at a rotor speed of 50 rpm at 200°C for 30 min mixing or at 240°C for 20 min of mixing, where the dark areas represent the PS phase and the light areas represent the PC phase. In Fig. 9 we observe that in the 30/70 PC/PS blend the minor component PC forms the discrete phase and the major component PS forms the continuous phase after mixing at 200°C for 30 min and the state of dispersion is slightly improved at 240°C. Since the viscosity of PS is much lower than that of PC at both 200°C and 240°C, and the less viscous PS is the major component, it is not surprising to observe that the 30/70 PC/PS blend gives rise to a dispersed morphology. Note that the melt blending temperature 200°C is very close to T_{cf} (200°C) of PC and about 45°C above T_{cf} (155°C) of PS. This consideration explains why at 200°C a very poorly mixed, co-continuous morphology is observed in the 70/30 PC/PS blend, in which the *major* component PC is expected to form the continuous phase and the *minor* component PS is expected to form the discrete phase. However, as the melt blending temperature is increased from 200°C to 240°C, the co-continuous morphology of the 70/30 PC/PS blend at 200°C is transformed into a dispersed morphology. This is attributable to the fact that the melt blending temperature of 240°C is much higher than the T_{cf}s of both PS and PC. A similar observation can be made for the 50/50 PC/PS blend, in which the more viscous PC forms the discrete phase and the less viscous PS forms the continuous phase.

Fig. 10 gives the SEM images of the 50/50 PC/PS blend at 200°C, describing the effect of rotor speed on morphology evolution. In Fig. 10 we observe a co-continuous morphology having a skeletal structure of PC after 5 min mixing, but the skeletal structure of PC began to break down, forming the discrete phase after 30 min mixing as the rotor speed increased from 10 to 150 rpm (i.e. as $\dot{\gamma}$ increased from 10.9 to $163.5\ s^{-1}$). This observation is very similar to that made earlier for the 60/40 PMMA/PS blend (see Fig. 7).

3.3. Morphology evolution in blends consisting of amorphous and crystalline polymers

3.3.1. PS/HDPE blends

The upper panel of Fig. 11 gives the log η versus log $\dot{\gamma}$ plots for PS and HDPE at 160°C, 180°C, 200°C, and 220°C for $\dot{\gamma} = 0.001$–$1000\ s^{-1}$, showing that the viscosity of PS is higher at 160°C and 180°C, but lower at 200°C and 220°C, than that of HDPE over a wide range of $\dot{\gamma}$; and that both PS and HDPE exhibit strong shear-thinning behavior. In order to facilitate our discussion later, the temperature dependence of viscosity ratio, η_{PS}/η_{HDPE}, at $\dot{\gamma} = 54.5\ s^{-1}$ is given in the lower panel of Fig. 11, showing that η_{PS}/η_{HDPE} ratio decreases from ca. 1.2 at 160°C, passing through 1.0 at ca. 185°C and then decreases further to 0.4 at 240°C. This information will be very useful to interpret morphology evolution in the PS/HDPE blends later.

Fig. 12 gives the SEM images of the 30/70 and 70/30 PS/HDPE blends, respectively, which were prepared at a rotor speed of 50 rpm for 30 min of mixing at 150°C, 160°C, or 220°C, where the dark areas represent the PS phase and the light areas represent the HDPE phase. The following observations are worth noting on the morphology evolution in the 30/70 PS/HDPE blend given in Fig. 12. At a mixing temperature of 150°C, the HDPE (the major component)

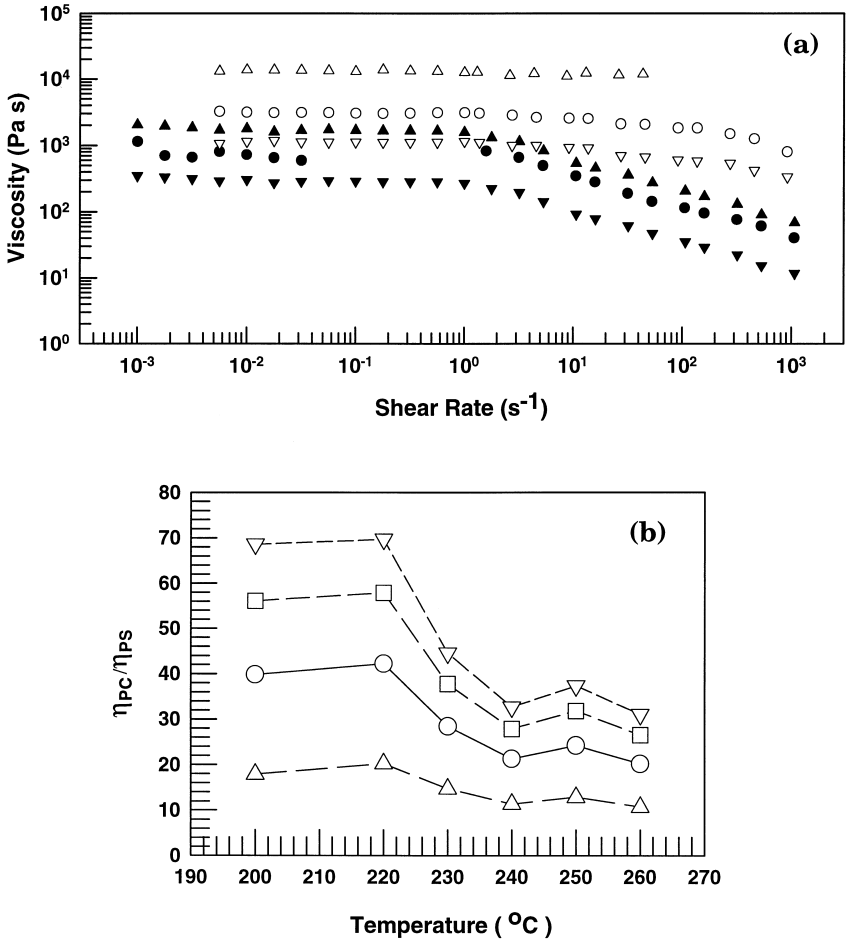

Fig. 8. (a) The upper panel describes the shear rate dependence of viscosity for PC (open symbols) and PS (filled symbols) at various temperatures: (○, ●) 220°C; (△, ▲) 240°C; (▽, ▼) 260°C. (b) The lower panel describes the temperature dependence of viscosity ratio, η_{PC}/η_{PS}, at various shear rates: (▽) 163.5 s^{-1}; (□) 109 s^{-1}; (○) 54.5 s^{-1}; (△) 10.9 s^{-1}.

having the T_m of 125°C forms the matrix phase because it already melted while PS (the minor component) shows a very irregularly shaped dispersed phase, indicating that the softening of PS was not complete. This can be interpreted as being the situation where the mixing temperature employed (150°C) is slightly below the $T_{cf} \approx 155$°C of PS. At a mixing temperature of 160°C, the dispersed state of the PS phase became quite different from that at 150°C, indicating that the discrete phase PS already began to flow at 160°C. At a mixing temperature of 220°C, we observe a well-developed dispersed morphology. Note that at 220°C the *major* component HDPE is more viscous than the *minor* component PS (see Fig. 11), indicating that the blend ratio is predominant over the viscosity ratio in determining morphology evolution in the 30/70 PS/HDPE blend.

The following observations are worth noting on the morphology evolution in the 70/30 PS/HDPE blend given in Fig. 12. At a mixing temperature of 150°C, we observe a co-continuous morphology in which interconnected structures of HDPE appear to be suspended in the yet unsoftend PS phase. The 70/30 PS/HDPE blend still shows a co-continuous morphology after mixing at 160°C for 30 min. As the mixing temperature is increased to 220°C we observe a well-developed dispersed morphology in which the *minor* component HDPE having higher viscosity forms the discrete phase and the *major* component PS having lower viscosity forms the continuous phase.

Fig. 13 gives the SEM images of the 50/50 PS/HDPE blend, which was prepared at a rotor speed of 50 rpm for 30 min mixing at 150°C, 160°C, 180°C, 200°C, 220°C, and 240°C. It is clear that at 150°C there is hardly any mixing, but at 180°C we observe a dispersed morphology in which the PS formed the dispersed phase and the HDPE formed the continuous phase. Interestingly enough, at 200°C we observe a co-continuous morphology and at 240°C we observe a breakdown of interconnected structures of HDPE that existed at 220°C, giving rise to a dispersed morphology in which the discrete phase of HDPE, though not so well developed, is dispersed in the continuous PS phase. In other words, we observe a phase inversion taking place in the 50/50 PS/HDPE blend as the mixing temperature is increased from 180°C to 240°C, passing through a co-continuous morphology at an intermediate temperature. We reason the occurrence of the phase inversion observed in the

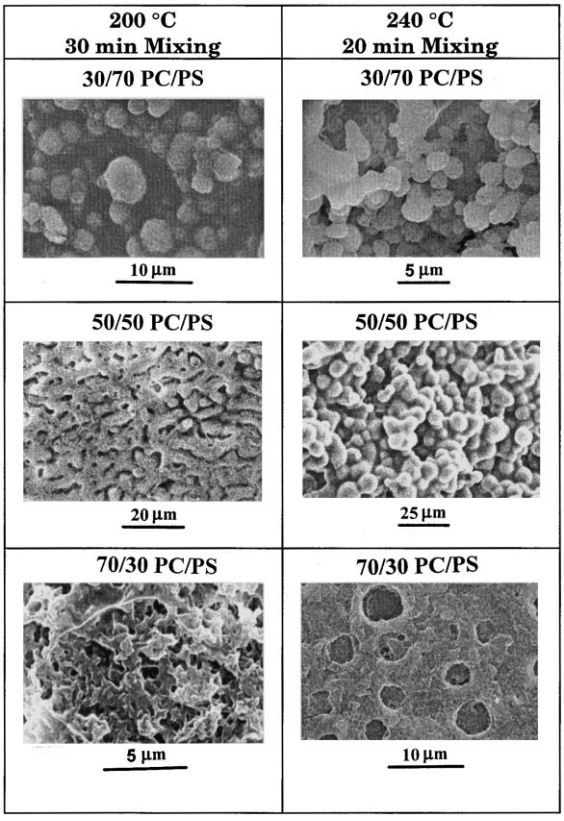

Fig. 9. SEM images describing the effect of melt blending temperature (200°C versus 240°C) on the morphology evolution in the 30/70, 50/50, and 70/30 PC/PS blends during compounding at a rotor speed of 50 rpm for 30 min at 200°C and 20 min at 240°C in a Brabender Plasticorder.

50/50 PS/HDPE blend as follows. With reference to Fig. 11, the viscosity of PS is higher than that of HDPE at temperatures below about 185°C, and thus the η_{PS}/η_{HDPE} ratio is slightly larger than 1 at 180°C but it decreases rapidly with increasing temperature and $\eta_{PS}/\eta_{HDPE} \approx 0.4$ at 240°C. The blend composition being equal in the 50/50 PS/HDPE blend, we conclude from Fig. 13 that the viscosity ratio determined the state of dispersion in the 50/50 PS/HDPE blend in that, the more viscous HDPE forms the discrete phase and the less viscous PS forms the continuous phase at $T \geq 240$°C.

Fig. 14 gives the SEM images of the 45/55 and 55/45 PS/HDPE blends, which were prepared at a rotor speed of 50 rpm for 3–5 min and 30 min of mixing at 220°C, showing that a co-continuous morphology persists even after 30 min of mixing in both blends. However, as can be seen in Fig. 15, as the melt blending temperature is increased from 220°C to 240°C and mixing is continued for 25 min, both the 45/55 and 55/45 PS/HDPE blends form a dispersed morphology in which the *major* component forms the continuous phase and the *minor* component forms the discrete phase. A transformation from a co-continuous morphology into a dispersed morphology in the 45/55 PS/HDPE blend is also realized, as can be seen in Fig. 16, when the rotor speed is increased from 50 to 150 rpm (compare with the upper panel of Fig. 14). In Fig. 16 we observe a

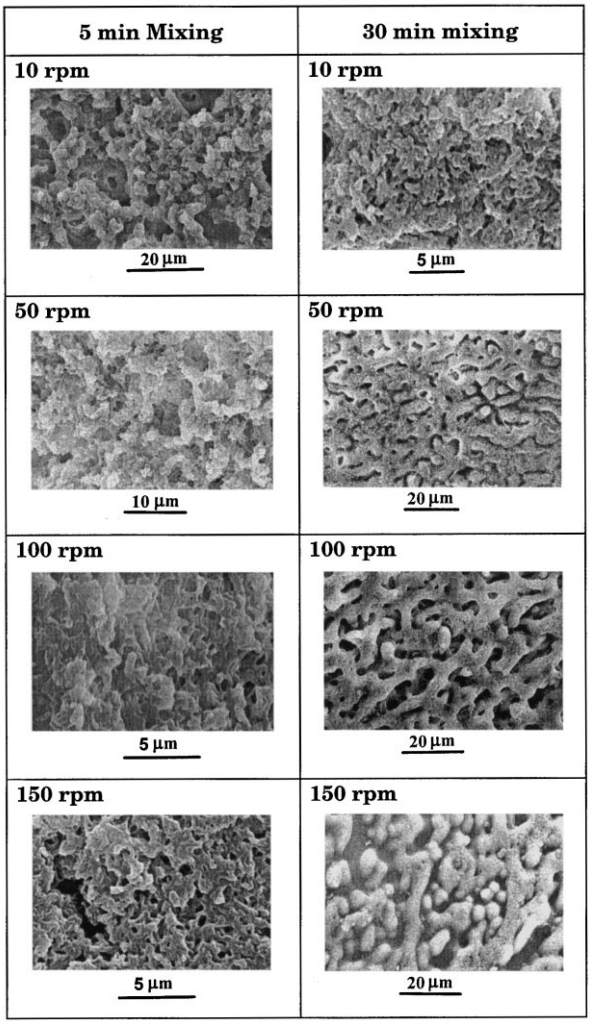

Fig. 10. SEM images describing the effect of rotor speed (10, 50, 100 or 150 rpm) and mixing time (5 versus 30 min) on the morphology evolution in the 50/50 PC/PS blend during compounding at 200°C in a Brabender Plasticorder.

clear picture about the morphology evolution in the 45/55 PS/HDPE blend as mixing time is increased from 5 to 30 min, leading us to conclude that a co-continuous morphology is not stable.

3.3.2. PS/PP blends

The upper panel of Fig. 17 gives the log η versus log $\dot{\gamma}$ plots for PS and PP at 190°C, 200°C, 220°C, and 240°C for $\dot{\gamma} = 0.001$–$1000\ s^{-1}$, showing that the viscosity of PS is higher at temperatures below about 184°C and lower at higher temperatures than that of PP over a wide range of $\dot{\gamma}$ tested, and that both PS and PP exhibit strong shear-thinning behavior. In order to facilitate our discussion later, the lower panel of Fig. 17 shows the temperature dependence of viscosity ratio, η_{PS}/η_{PP}, at $\dot{\gamma} = 54.5\ s^{-1}$. This information will be very useful to interpret morphology evolution in the PS/PP blends later.

Fig. 18 gives the SEM images of the 30/70 and 70/30

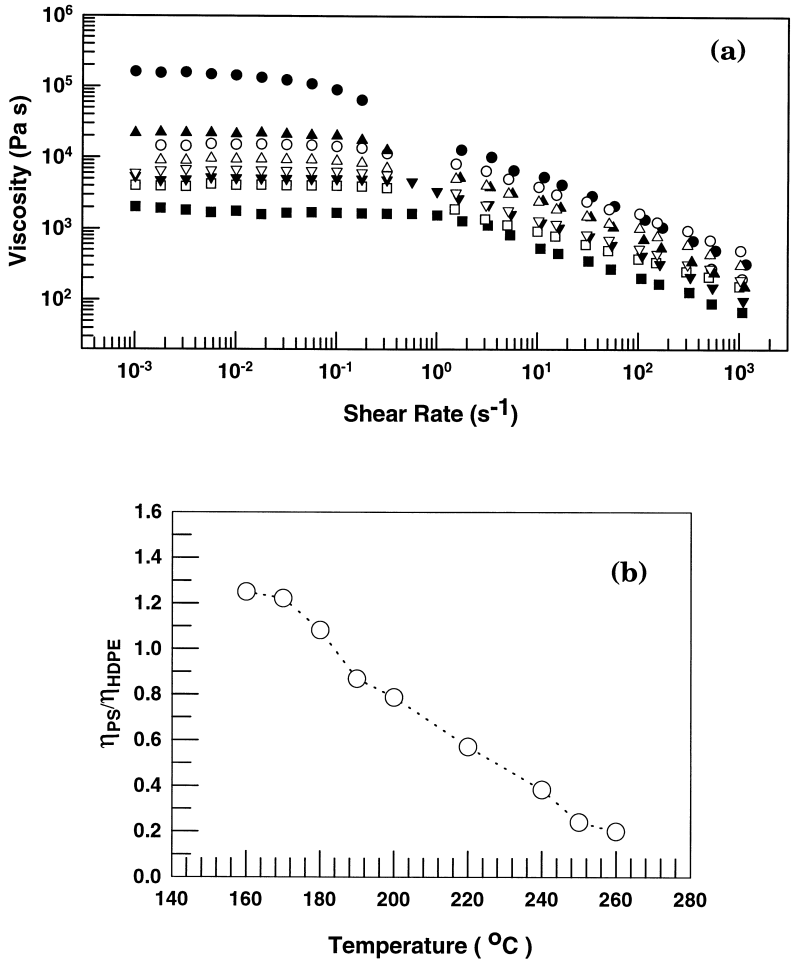

Fig. 11. (a) The upper panel describes the shear rate dependence of viscosity for HDPE (open symbols) and PS (filled symbols) at various temperatures: (○, ●) 160°C; (△, ▲) 180°C; (▽, ▼) 200°C; (□, ■) 220°C. (b) The lower panel describes the temperature dependence of viscosity ratio, η_{PS}/η_{HDPE}, at $\dot{\gamma} = 54.5\ s^{-1}$.

PS/PP blends, respectively, which were prepared at a rotor speed of 50 rpm for 30 min of mixing at 175°C, 190°C, 220°C, and 240°C, where the dark areas represent the PS phase and the light areas represent the PP phase. The following observations are worth noting on the 30/70 PS/PP blend given in Fig. 18. At 175°C we observe very irregularly shaped discrete phase of PS dispersed in interconnected structures of the PP phase in the 30/70 PS/PP blend. This can be interpreted as being the situation where the mixing temperature employed (175°C) is only 10°C above the T_m of PP and thus PS and PP did not have good mixing although PS having $T_{cf} = 155$°C might have acted as 'liquid'. Note that T_{cf} (PS) $< T_m$ (PP) in the PS/PP blends, whereas T_{cf} (PS) $> T_m$ (HDPE) in the PS/HDPE blends considered earlier. At 190°C we observe a much improved morphology in the 30/70 PS/PP blend, in which PS forms the discrete phase and PP forms the continuous phase. At 220°C and 240°C we observe a well-developed dispersed morphology in the 30/70 PS/PP blend. It should be remembered that at 220°C and 240°C the *major* component PP is more viscous than the *minor* component PS (see Fig. 16), indicating that the blend ratio is predominant over the viscosity ratio in determining morphology evolution in the 30/70 PS/PP blend, very similar to that observed in the 30/70 PS/HDPE blend (see Fig. 12).

The following observations are worth noting in the 70/30 PS/PP blend given in Fig. 18. At 175°C we observe interconnected structures of PP suspended in the PS phase. At 190°C we observe a breakdown of interconnected structures of PP, and at 240°C we observe a well-developed dispersed morphology, in which the *minor* component PP having higher viscosity forms the discrete phase and the *major* component PS having lower viscosity forms the continuous phase. Again, this observation is consistent with that observed in the 70/30 PS/HDPE blend (see Fig. 12).

Fig. 19 gives the SEM images of the 50/50 PS/PP blend, which was prepared at a rotor speed of 50 rpm for 5 and 30 min of mixing at 175°C, 190°C, 220°C, and 240°C. In Fig. 19 we observe a co-continuous morphology regardless of whether the 50/50 PS/PP blend was mixed for 5 or 30 min at temperatures ranging from 175°C to 240°C. This observation is different from that made in the 50/50 PS/HDPE blend (see Fig. 13) that underwent a phase inversion at a temperature between 180°C and 240°C.

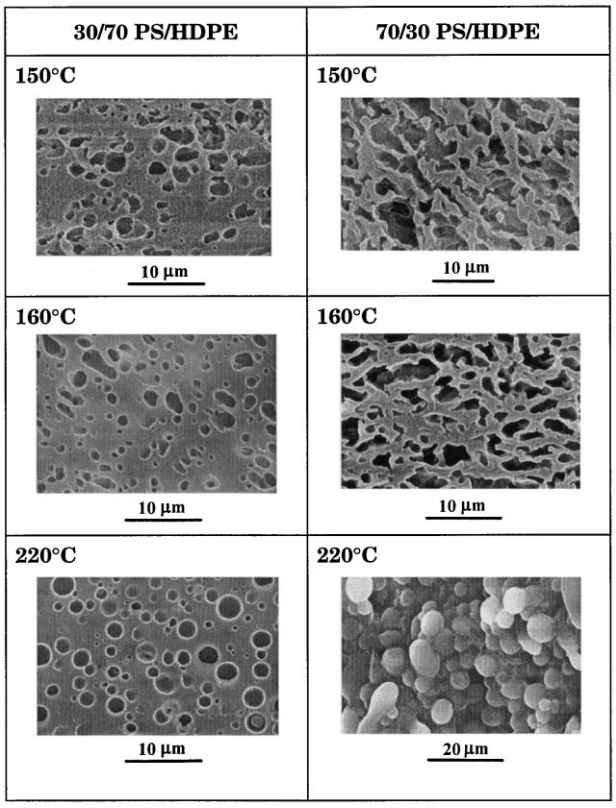

Fig. 12. SEM images describing the effect of melt blending temperature (150°C, 160°C, or 220°C) on the morphology evolution in the 30/70 and 70/30 PS/HDPE blends during compounding at a rotor speed of 50 rpm for 30 min in a Brabender Plasticorder.

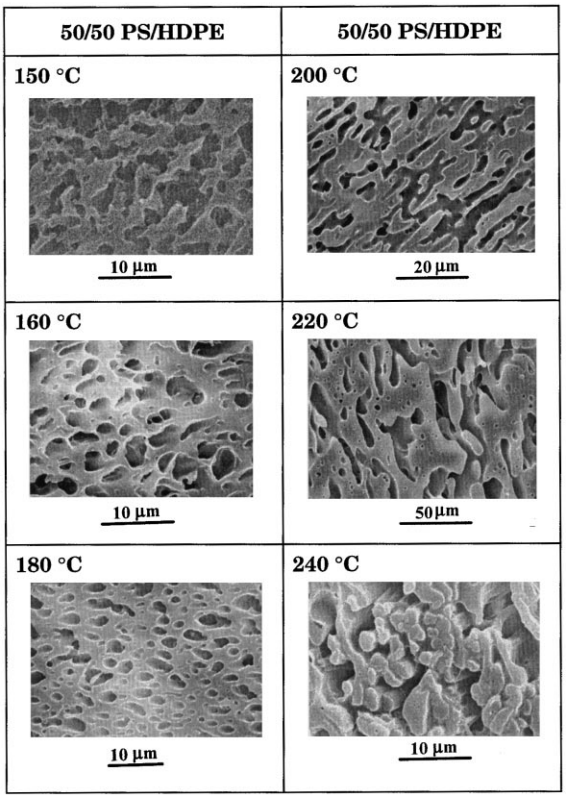

Fig. 13. SEM images describing the effect of melt blending temperature (150°C, 160°C, 180°C, 200°C, 220°C, or 240°C) on the morphology evolution in the 50/50 PS/HDPE blend during compounding at a rotor speed of 50 rpm for 30 min in a Brabender Plasticorder.

Fig. 20 gives the SEM images of the 50/50 PS/PP blend that was prepared (i) at 240°C and a rotor speed of 150 rpm (the left panel) or (ii) at 260°C and a rotor speed of 50 rpm (the right panel) for 5, 10, and 20 min of mixing. In Fig. 20 we observe that at 240°C and a rotor speed of 150 rpm a co-continuous morphology persists even after 20 min mixing although interconnected structures of PP broke down somewhat, but at 260°C and a rotor speed of 50 rpm interconnected structures of PP break down completely to form a well-developed dispersed morphology in which the *more* viscous PP forms the discrete phase and the *less* viscous PS forms the continuous phase. The above observation indicates that the formation of a dispersed morphology in the 50/50 PS/PP blend requires a higher mixing temperature compared to the 50/50 PS/HDPE blend (compare Fig. 20 with Fig. 13) and that the co-continuous morphology observed in the 50/50 PS/PP blend at temperatures below 260°C is not stable.

In order to investigate the morphology evolution as affected by the intensity of mixing, we varied the rotor speed ranging from 10 to 150 rpm for the 45/55 PS/PP blend at a mixing temperature of 220°C. The SEM images of the 45/55 PS/PP blend are given in Fig. 21 for a rotor speed of 10 rpm, in Fig. 22 for a rotor speed of 50 rpm, in Fig. 23 for a rotor speed of 100 rpm, and in Fig. 24 for a

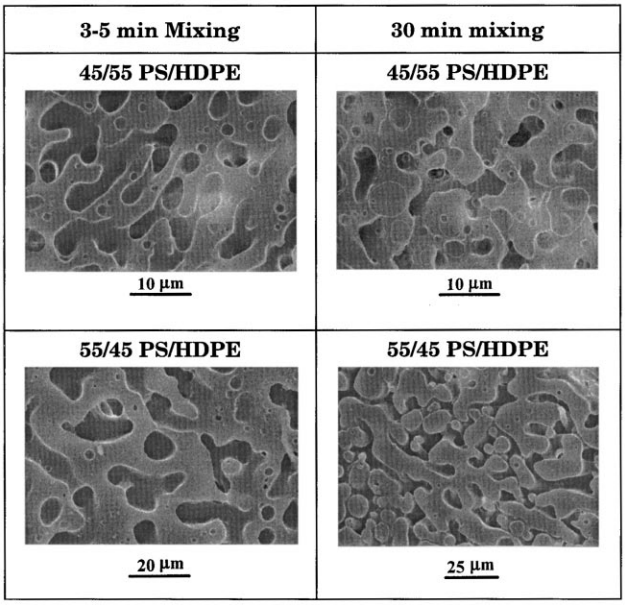

Fig. 14. SEM images describing the effect of mixing time (3–5 versus 30 min) on the morphology evolution in the 45/55 and 55/45 PS/HDPE blends during compounding at a rotor speed of 50 rpm and at 220°C in a Brabender Plasticorder.

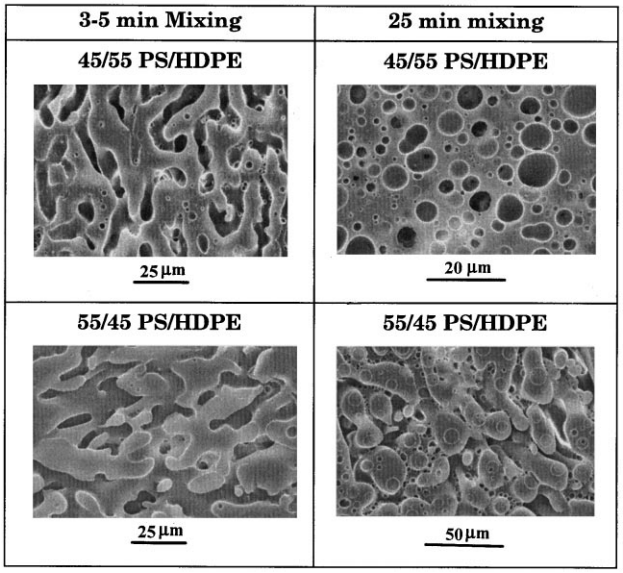

Fig. 15. SEM images describing the effect of mixing time (3–5 versus 30 min) on the morphology evolution in the 45/55 and 55/45 PS/HDPE blends during compounding at a rotor speed of 50 rpm and at 240°C in a Brabender Plasticorder.

rotor speed of 150 rpm. In Figs. 21–24 we observe that a co-continuous morphology eventually transforms into a dispersed morphology when mixing is carried out for a sufficiently long time: (i) after 90 min mixing at a rotor speed of 10 rpm, (ii) after 60 min mixing at a rotor speed of 50 rpm, (iii) after 45 min mixing at a rotor speed of 100 rpm, and (iv) after 30 min mixing at a rotor speed of 150 rpm. That is, the higher the rotor speed (i.e. the greater the intensity of mixing), the shorter the mixing time would be for a transformation from a co-continuous morphology to a dispersed morphology to occur.

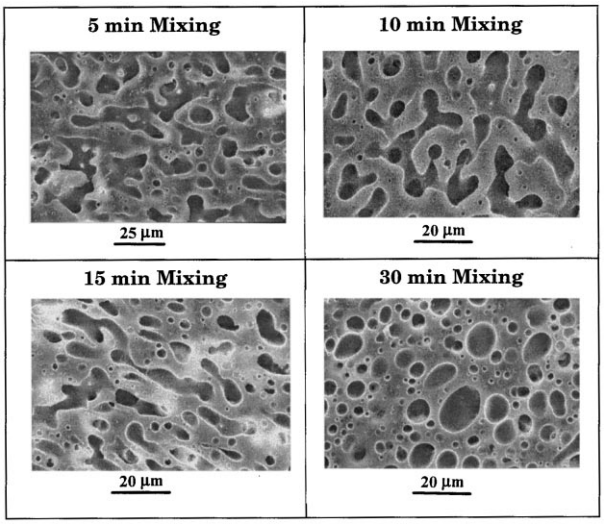

Fig. 16. SEM images describing the effect of mixing time (5, 10, 15, and 30 min) on the morphology evolution in the 45/55 PS/HDPE blend during compounding at a rotor speed of 150 rpm and 220°C in a Brabender Plasticorder.

4. Discussion

4.1. The significance of T_{cf} of an amorphous polymer in the formation of blend morphology during compounding

In this paper we have shown that the conventional view that the T_g of an amorphous polymer may be regarded as being equivalent to the softening temperature cannot explain the morphology of a binary polymer blend, consisting of two amorphous polymers (PMMA/PS or PC/PS blends) or consisting of an amorphous polymer and a crystalline polymer (PS/HDPE or PS/PP blends), that was prepared at temperatures below or at slightly above T_g. However, we were able to explain the experimental results using the concept of T_{cf} [15]. This is very significant in that the initial morphology of a polymer blend is dictated by the difference between two T_{cf}s when preparing a binary blend consisting of two amorphous polymers or by the difference between T_{cf} and T_m when preparing a binary blend consisting of an amorphous polymer and a crystalline polymer.

We have shown above that a polymer blend prepared at temperatures below the T_{cf} of an amorphous polymer(s), owing to the very high viscosities, forms a co-continuous morphology regardless of blend composition. However, when a blend was prepared at temperatures much higher than the T_{cf} of an amorphous polymer(s) or by allowing for a sufficiently long mixing time, we observed a dispersed morphology. Such an observation is very similar to the morphological transformation from a co-continuous morphology to a dispersed morphology, which was observed during isothermal annealing of a rapidly precipitated PMMA/PS blend [16].

4.2. Stability of the co-continuous morphology observed during melt blending

A fundamental question may be raised as to whether or not a co-continuous morphology often observed in immiscible polymer blends is stable. The experimental results presented above lead us to conclude that a co-continuous morphology is not stable and it is rather a transitory morphology that appears when one type of dispersed morphology (droplets of component A are dispersed in the matrix phase of B) is transformed into another type of dispersed morphology (droplets of component B are dispersed in the matrix phase of A), i.e. when a phase (or matrix) inversion takes place during compounding.

Earlier, Miles and Zurek [7] noted that a co-continuous morphology was first observed when a 53/47 PS/PMMA blend was melt blended in a Brabender Plasticorder at 200°C at a rotor speed of 20 rpm that was equivalent to a shear rate of about $90\ s^{-1}$ and then the co-continuous morphology transformed into a dispersed morphology when the melt-blended specimen was extruded further through a capillary rheometer at a shear rate of $27\ s^{-1}$. Based on this observation, they concluded that a

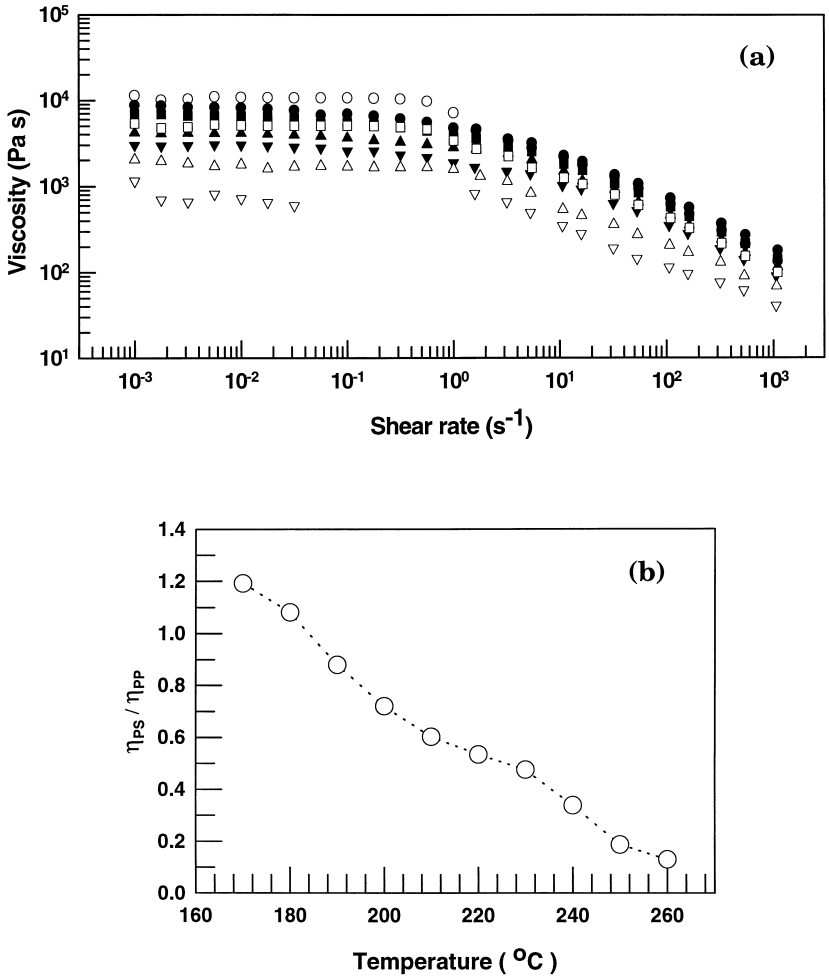

Fig. 17. (a) The upper panel describes the shear rate dependence of viscosity for PS (open symbols) and PP (filled symbols) at various temperatures: (○, ●) 190°C; (□, ■) 200°C; (△, ▲) 220°C; (▽, ▼) 240°C. (b) The lower panel describes the temperature dependence of viscosity ratio, η_{PS}/η_{PP}, at $\dot{\gamma} = 54.5\ s^{-1}$.

co-continuous morphology was not stable. However, the experiment of Miles and Zurek is *not* conclusive in that the co-continuous morphology initially formed in a Brabender Plasticorder must have been altered, if not destroyed completely, while the blend specimen was heated inside the barrel of the capillary rheometer (i.e. even before it was subjected to extrusion).

More recently, in investigating the formation of a co-continuous morphology in nylon 6-polyethersulfone and poly(butylene terephthalate)-polystyrene blend systems, respectively, He et al. [10] observed that the range of blend ratio over which a co-continuous morphology formed became narrower as the mixing time was increased and then speculated that after a sufficiently long mixing time a co-continuous morphology would have occurred at an equal blend composition (50/50 blend ratio). Such experimental results indicate that a co-continuous morphology would not occur necessarily at an equal blend composition and it can be made to disappear at high enough melt blending temperature or after a sufficiently long mixing time.

In the present study we have observed a co-continuous morphology over a blend ratio ranging from 40/60 to 60/40 in the PS/PP blends when melt blending was conducted at 220°C at a rotor speed of 50 rpm, but this range became narrower as the mixing temperature was increased to 240°C. Specifically, the 45/55 PS/PP blend which formed a co-continuous morphology at 220°C transformed into a dispersed morphology as the mixing temperature was increased to 240°C under otherwise identical processing conditions.

One of the most significant findings in the present study is that prolonging the mixing time at a given rotor speed or increasing the rotor speed (i.e. the intensity of mixing or shear rate applied) for a fixed mixing time transforms a co-continuous morphology into a dispersed morphology. Specifically, we found that for the 45/55 PS/PP blend, a co-continuous morphology transformed into a dispersed morphology when the mixing continued (i) for approximately 90 min at a rotor speed of 10 rpm (Fig. 21), (ii) for approximately 60 min at a rotor speed of 50 rpm (Fig. 22), (iii) for approximately 45 min at a rotor speed of 100 rpm (Fig. 23), or (iv) for approximately 30 min at a rotor speed

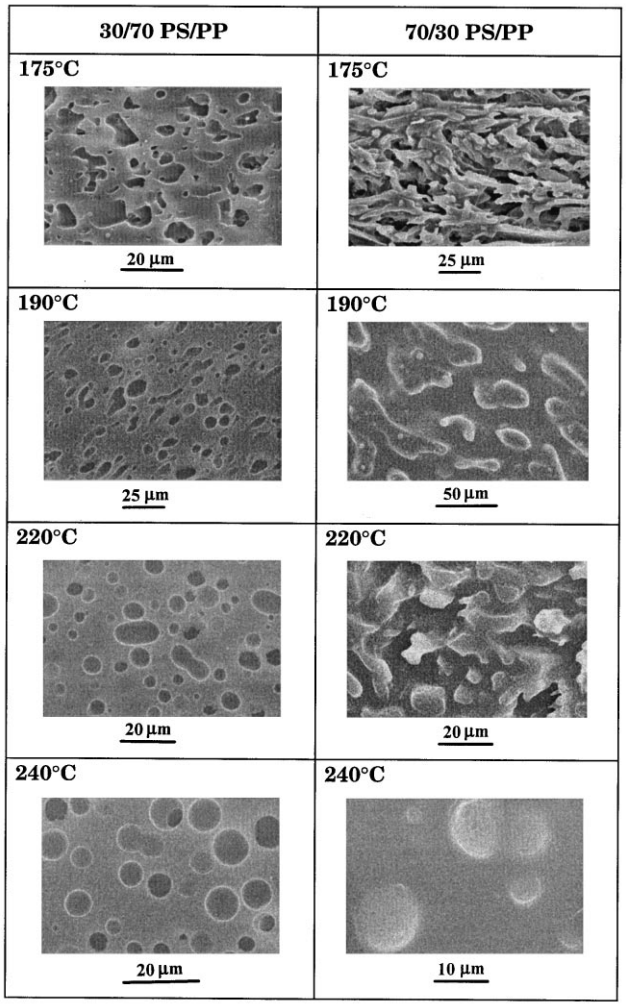

Fig. 18. SEM images describing the effect of melt blending temperature (175°C, 190°C, 220°C, and 240°C) on the morphology evolution in the 30/70 and 70/30 PS/PP blends during compounding at a rotor speed of 50 rpm for 30 min in a Brabender Plasticorder.

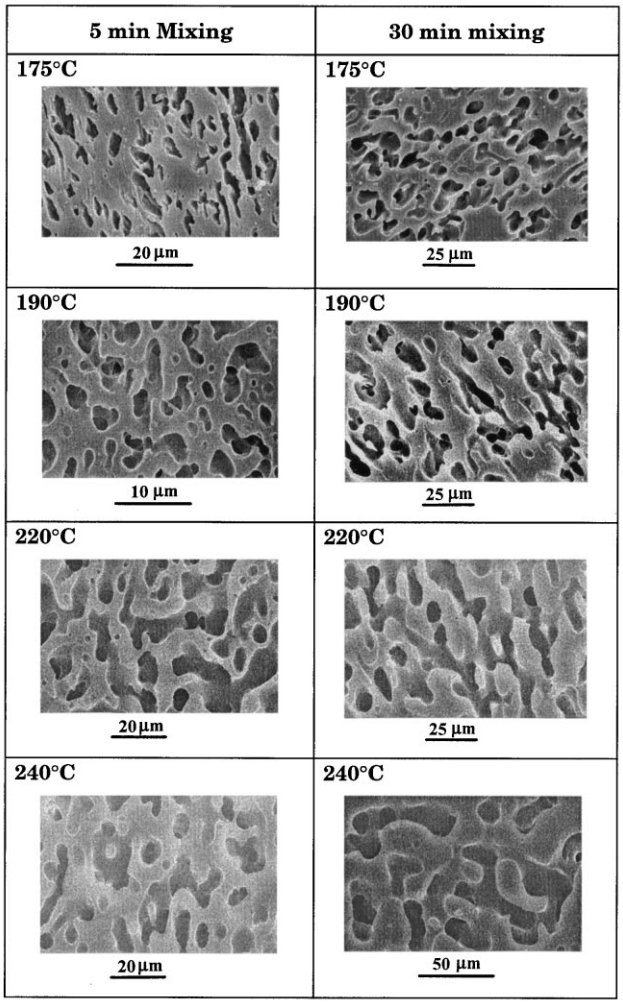

Fig. 19. SEM images describing the effect of mixing time (5 versus 30 min) and melt blending temperature (175°C, 190°C, 220°C, and 240°C) on the morphology evolution in the 50/50 PS/PP blend during compounding at a rotor speed of 50 rpm in a Brabender Plasticorder.

of 150 rpm (Fig. 24). The above results lead us to conclude that a co-continuous morphology represents a *transitory* morphological state for a phase transition from one type of dispersed morphology (where the discrete phase A dispersed in the continuous phase B) to another type of dispersed morphology (where the discrete phase B dispersed in the continuous phase A).

We have recorded, during compounding of each blend investigated in this study, both the torque and mechanical energy on a Brabender Plasticorder. Fig. 25(a) (the upper panel) gives variations of torque with mixing time, during compounding of the 45/55 PS/PP blend at 220°C, at four different rotor speeds: 10, 50, 100, and 150 rpm. It can be seen in Fig. 25(a) that the torque goes through a maximum within a few minutes after melt blending began and then decreases rapidly, giving rise to a more or less constant value for the remaining period of mixing for 30 min. It should be mentioned that the peak value of torque observed in Fig. 25(a) is due to the initial mixing of two polymers in the solid state and thus the torque decreases rapidly once the melting or softening of the polymers begins. It is worth noting in Fig. 25(a) that the values of torque are relatively insensitive to the rotor speed (10–150 rpm) of a Brabender Plasticorder. However, as can be seen in Fig. 25(b) (the lower panel), the mechanical energy applied to the blend by the Brabender Plasticorder is very sensitive to the rotor speed, namely, the mechanical energy increases with increasing rotor speed from 10 to 150 rpm: the higher the rotor speed of the mixing equipment, the greater is the mechanical energy applied to the blend. It should be mentioned that values of the mechanical energy plotted in Fig. 25(b) were read off from the Brabender Plasticorder. According to the manufacturer of the Brabender Plasticorder, the mechanical energy was calculated from the area under the torque versus time curve (see Fig. 25(a)) multiplied by 2πRPM with RPM being rotor speed. Fig. 25(b) seems to explain the experimental results given

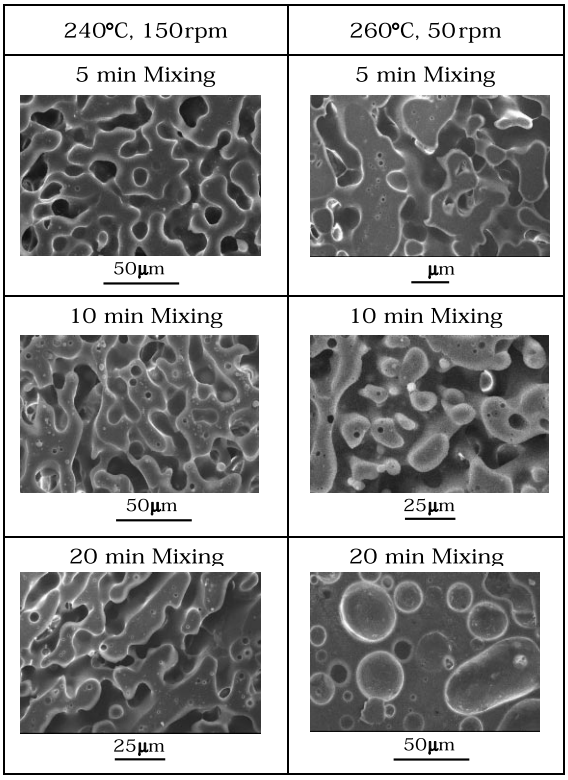

Fig. 20. SEM images describing the effect of melt blending temperature (240°C versus 260°C), rotor speed (150 versus 50 rpm), and mixing time (5, 10, and 20 min) on the morphology evolution in the 50/50 PS/PP blend during compounding in a Brabender Plasticorder.

in Figs. 21–24, i.e. the reason why a shorter mixing time was required to transform a co-continuous morphology into a dispersed morphology as the rotor speed was increased from 10 to 150 rpm. It appears from Fig. 25 that there exists

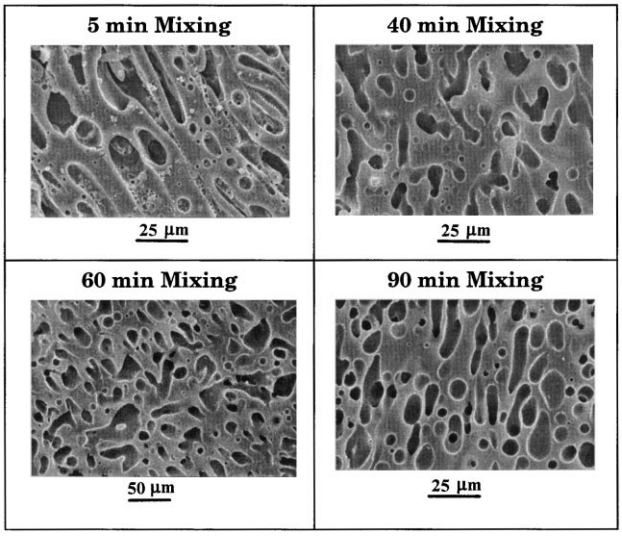

Fig. 21. SEM images describing the effect of mixing time (5, 40, 60, and 90 min) on the morphology evolution in the 45/55 PS/PP blend during compounding at a rotor speed of 10 rpm and at 220°C in a Brabender Plasticorder.

a critical value of mechanical energy that is required to transform a co-continuous morphology into a dispersed morphology. The critical value of mechanical energy would depend on the characteristics of a pair of polymers being melt blended and the blend ratio.

4.3. Factors affecting a phase inversion during melt blending

From the point of view of the principle of minimum energy dissipation in channel flow of two immiscible liquids, the component having lower viscosity is expected to form the continuous phase, wetting the channel wall where the shear stress is greatest. In this regard, for example, the 70/30 PMMA/PS blend investigated in this study should have a dispersed morphology where the more viscous PMMA forms the discrete phase and the less viscous PS forms the continuous phase. But our experimental results show the opposite trend. In all the five blend systems investigated in this study, we observed that the *major* component forms the continuous phase and the *minor* component forms the discrete phase, irrespective of the viscosity ratio of the constituent components. In contrast, we observed that for blends having an equal volume fraction, the *more viscous* component forms the discrete phase and the *less viscous* component forms the continuous phase, which is in good agreement with the principle of minimum energy dissipation. The earlier observations suggest that a very delicate relationship, which controls the state of dispersion in an immiscible polymer blend, exists between volume fraction and viscosity ratio.

By attaching glass windows to the wall of an internal mixer to record the morphology development during melt blending, Shih [11] and Sundararaj et al. [12] observed that initially, the minor phase, which had a lower *softening* temperature compared to the major component, formed the continuous phase and coated the major component, and as the major component melted, a phase inversion occurred and thus the major component became the continuous phase. Then, they concluded that a phase inversion would occur during melt blending when the softening or melting transition temperature of the minor component is lower than that of the major component. Such a conclusion may be valid when the viscosity of the major component is lower than that of the minor component, but *not* when the viscosity of the major component is much higher than that of the minor component, as borne out to be case in the present study. In dealing with a blend consisting of an amorphous polymer and a crystalline polymer, Shih and co-workers [11,12] did *not* elaborate on what might be the softening temperature of the amorphous polymer.

In this study we measured the rheological properties of the individual polymers at various temperatures and shear rates, comparable to the processing conditions employed in the melt blending experiments conducted in a Brabender Plasticorder and correlated the viscosity ratio of the

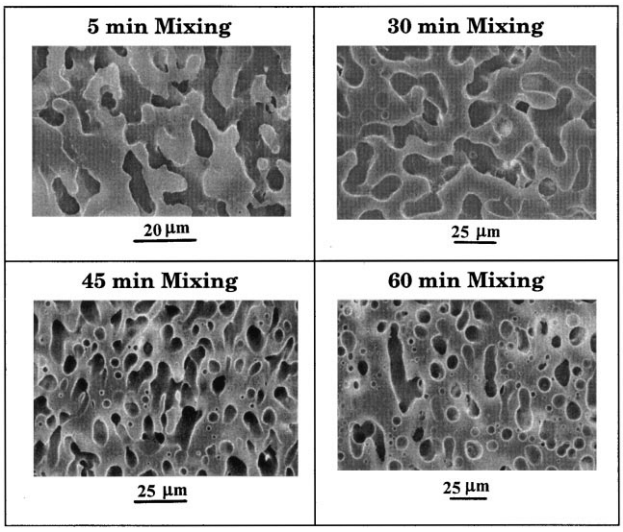

Fig. 22. SEM images describing the effect of mixing time (5, 30, 45, and 60 min) on the morphology evolution in the 45/55 PS/PP blend during compounding at a rotor speed of 50 rpm and at 220°C in a Brabender Plasticorder.

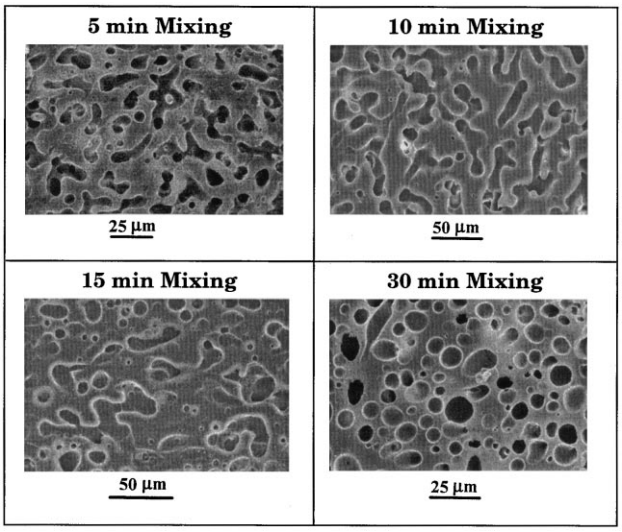

Fig. 24. SEM images describing the effect of mixing time (5, 10, 15, and 30 min) on the morphology evolution in the 45/55 PS/PP blend during compounding at a rotor speed of 150 rpm and at 220°C in a Brabender Plasticorder.

constituent components at a particular temperature and strain rate of interest to the evolution of blend morphology. We have shown that during compounding, a phase inversion may take place (1) when a component having higher T_m or T_{cf}, which initially formed the discrete phase, has a viscosity lower than the other component for symmetric or nearly symmetric blend compositions after the melt blending temperature is increased far above the T_m or T_{cf} of both components; (2) regardless of the viscosity ratio, when a component having higher T_m or T_{cf}, which initially formed the discrete phase, is the major component after the melt blending temperature is increased far above the T_m or T_{cf} of both components; or (3) when the viscosity ratio of the constituent components having symmetric or nearly symmetric blend composition reverses as the temperature is increased far above the T_m or T_{cf} of both components. The present study indicates that for symmetric or nearly symmetric blend compositions, the viscosity ratio of the constituent components plays a predominant role in determining the state of dispersion (or phase inversion) during melt blending. Figs. 26 and 27 give a summary of our experimental results, describing relationships between blend ratio and viscosity ratio, for the PS/HDPE and PS/PP blends, respectively.

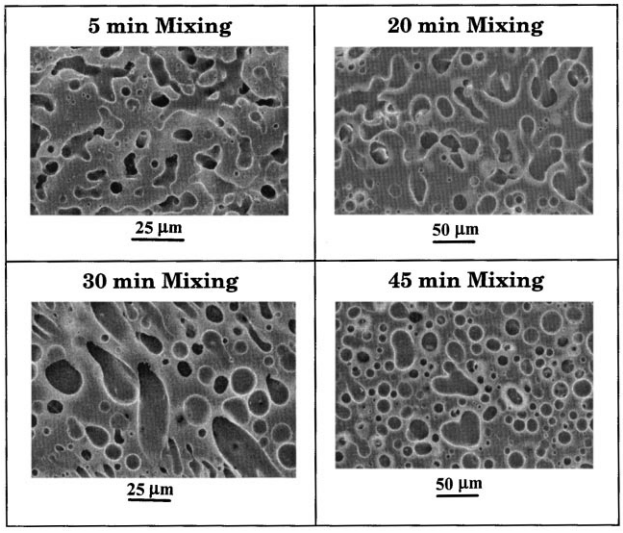

Fig. 23. SEM images describing the effect of mixing time (5, 20, 30, and 45 min) on the morphology evolution in the 45/55 PS/PP blend during compounding at a rotor speed of 100 rpm and at 220°C in a Brabender Plasticorder.

Based on the experimental observation made earlier by Han and Kim [2] that a co-continuous morphology having interconnected structures has a viscosity much higher than a dispersed morphology, we speculate that a certain amount of work (or mechanical energy) is required to overcome the barrier that separates one mode of dispersed morphology from another mode of dispersed morphology in two-phase polymer blends. Such a speculation appears to be supported by the experimental observations by Shih [11] and Sundararaj et al. [12] that torque went through a maximum during compounding when a phase inversion took place.

4.4. Effect of fluid elasticity on the mode of dispersion during compounding of two immiscible polymers

In 1974 van Oene [17] argued that the second normal stress difference (N_2) may play an important role in determining the morphology of immiscible polymer blends. Since then, however, little experimental evidence has been reported to either support or question van Oene's argument, because measurement of N_2 for polymer melts is difficult, especially at high shear rates. There are different ways of

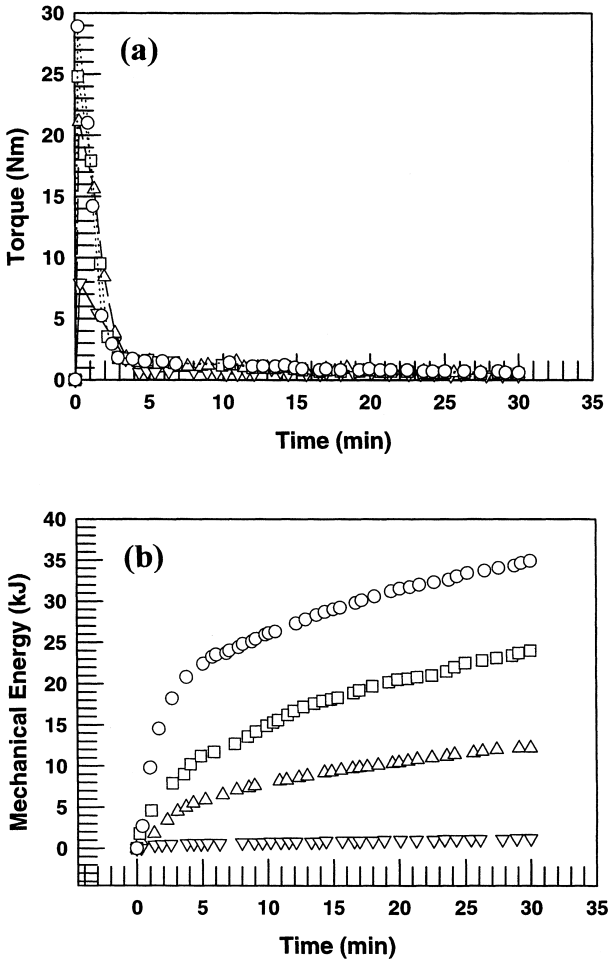

Fig. 25. (a) The upper panel describes the torque recorded on a Brabender Plasticorder during compounding of the 45/55 PS/PP blend at 220°C for various rotor speeds: (▽) 10 rpm, (△) 50 rpm, (□) 100 rpm, and (○) 150 rpm. (b) The lower panel describes the mechanical energy recorded on a Brabender Plasticorder during compounding of the 45/55 PS/PP blend at 220°C for various rotor speeds: (▽) 10 rpm, (△) 50 rpm, (□) 100 rpm, and (○) 150 rpm.

representing the elastic properties of polymers. According to Han [18–20], the elastic properties of polymeric liquids can be evaluated from $\log G'$ versus $\log G''$ plot, where G' is the storage modulus and G'' the loss modulus that can be easily determined from dynamic frequency sweep experiments. Note that G' represents the energy stored and G'' represents the energy dissipated per unit volume of fluid during oscillatory shear flow.

Fig. 28 gives the $\log G'$ versus $\log G''$ plots for PMMA and PS employed in this study at various temperatures. What is remarkable in Fig. 28 is that the $\log G'$ versus $\log G''$ plot is independent of temperature, which was first reported by Han and Lem [18] in 1982. It should be mentioned that the temperature independence of the $\log G'$ versus $\log G''$ plot has as its basis a molecular viscoelasticity theory for monodisperse homopolymers [19] and also for polydisperse homopolymers [20,21]. Following

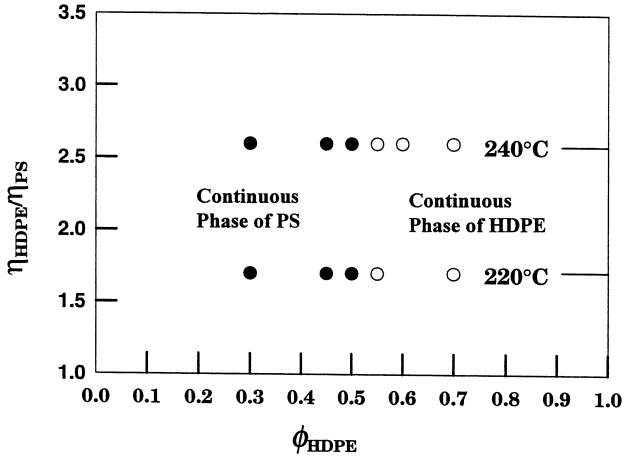

Fig. 26. Effect of blend composition and viscosity ratio on the mode of dispersed morphology for the PS/HDPE blends at 220°C and 240°C. Filled circle (●) denotes a dispersed morphology in which HDPE forms the discrete phase and PS forms the continuous phase. Open circle (○) denotes a dispersed morphology in which PS forms the discrete phase and HDPE forms the continuous phase.

Han's rheological interpretation [18–21] we observe from Fig. 28 that PS is more elastic than PMMA, independent of temperature. This observation suggests that the elasticity ratio of PMMA and PS in a PMMA/PS blend remained constant regardless of the mixing temperature employed, while the viscosity ratio of PMMA and PS varied with mixing temperature. It should be pointed out that $\log G'$ versus $\log G''$ plot has *no* relation whatsoever to the Cole–Cole plot [22], which uses rectangular coordinates showing temperature dependence on a semi-circle. Moreover, the Cole–Cole plot has no theoretical basis and it is strictly an empirical correlation.

In view of the fact that the morphological state of a

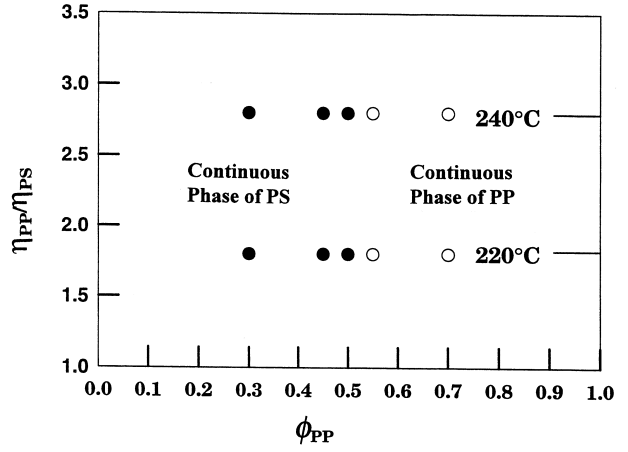

Fig. 27. Effect of blend composition and viscosity ratio on the mode of dispersed morphology for the PS/PP blends at 220°C and 240°C. Filled circle (●) denotes a dispersed morphology in which PP forms the discrete phase and PS forms the continuous phase. Open circle (○) denotes a dispersed morphology in which PS forms the discrete phase and PP forms the continuous phase.

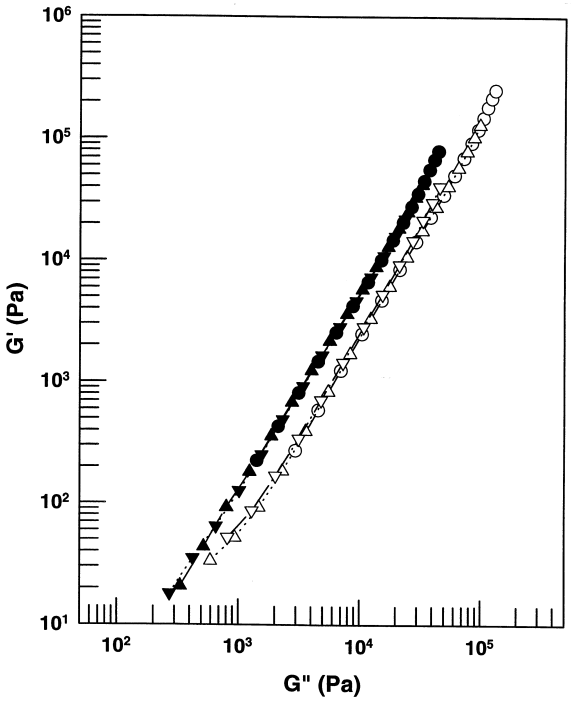

Fig. 28. The log G' versus log G'' plots for PMMA at 200°C (○), 220°C (△), 240°C (▽), and for PS at 180°C (●), 200°C (▲), and 220°C (▼).

PMMA/PS blend changed with mixing temperature, we conclude that the observed variations of blend morphology with mixing temperature were due to a change in viscosity ratio and the fluid elasticity played *little* role in determining the state of dispersion for the PMMA/PS blends *during compounding* in a Brabender Plasticorder. Using the log G' versus log G'' plots (not shown here for the reason of space limitation) for the PC/PS, PS/HDPE, PS/PP, and nylon 6/HDPE blend systems investigated in this study, we have reached the same conclusion as for the PMMA/PS blends, insofar as the role of fluid elasticity is concerned in determining the state of dispersion. We believe, however, that fluid elasticity would play a very important role in determining the size of the dispersed phase via droplet breakup and/or coalescence during compounding or during post-processing (e.g. extrusion or injection molding). This subject will be dealt with in a future publication.

5. Concluding remarks

In this paper we have investigated the evolution of polymer blend morphology during compounding in a batch mixer. We have pointed out that although from a thermodynamic point of view an amorphous polymer may be regarded as 'liquid' at temperatures above its T_g, from a rheological point of view it cannot be regarded as 'liquid' until the temperature is increased far above its T_g. In interpreting the morphology evolution in blends consisting of two amorphous polymers (PMMA/PS and PC/PS) or consisting of an amorphous polymer and a crystalline polymer (PS/HDPE and PS/PP blends), we used the concept of 'critical flow temperature' first introduced by Han [15]: $T_{cf} \cong T_g + 55$°C.

The morphology evolution based on the present study is summarized schematically in Fig. 29, where an immiscible blend consisting of two crystalline polymers is considered. When dealing with an immiscible blend consisting of two amorphous polymers or consisting of an amorphous polymer and a crystalline polymer, T_m in Fig. 29 should be replaced by T_{cf} for the amorphous polymer(s). With reference to Fig. 29, the T_m (or T_{cf}) of the constituent components plays an important role in the morphology evolution of an immiscible polymer blend. When the melt blending

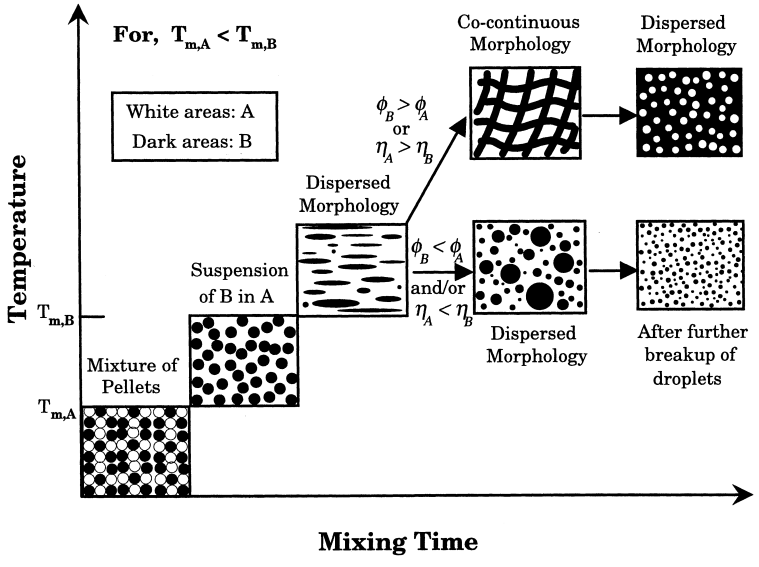

Fig. 29. Schematic describing the evolution of blend morphology during compounding of two immiscible polymers in an internal mixer, where the melting point of polymer A is assumed to be lower than that of polymer B.

temperature T lies between two T_ms or between two T_{cf}s of the constituent components (say $T_{m,A} < T < T_{m,B}$ or $T_{cf,A} < T < T_{cf,B}$), component A first forms the matrix phase in which component B, still in the solid state, is suspended, forming a suspension. When $T > T_{m,A} > T_{m,B}$ or $T > T_{cf,A} > T_{cf,B}$, initially a dispersed two-phase liquid forms having droplets of component B dispersed in the continuous (matrix) phase of component A. At this temperature, if the viscosity of component B is lower than that of component A (i.e. $\eta_B < \eta_A$) and/or component B is the major component, phase inversion may take place having component B as the continuous phase and component A as the discrete phase. When phase inversion takes place, as pointed out above, the two-phase liquid must pass through the transitory morphological state, a co-continuous phase.

We have shown that during melt blending in an internal mixer, the morphology of binary blends of immiscible polymers depends, among many factors, on (i) the melt blending temperature relative to the T_m of a crystalline polymer component and T_{cf} of an amorphous polymer component, (ii) rotor speed (i.e. the intensity of mixing), (iii) duration of mixing, (iv) viscosity ratio of the constituent components, and (v) blend composition. We demonstrated that a co-continuous morphology may be formed, irrespective of blend composition, when the melt blending temperature is lower than T_{cf} of the constituent component(s). However, a co-continuous morphology may be transformed into a dispersed morphology when the melt blending temperature is much higher than the T_{cf}. In such a situation the mode of dispersed morphology depends on blend composition and viscosity ratio, provided that a sufficiently long mixing time is allowed. If mixing time is *not* sufficiently long, one may end up with a co-continuous morphology, which certainly is *not* stable. We have shown that a co-continuous morphology is a transitory morphological state between two modes of dispersed morphology. We have shown further that if a sufficient time is allowed for melt blending or a proper processing condition (e.g. temperature) is chosen, a co-continuous morphology may be transformed into a dispersed morphology.

We would like to mention that breakup and coalescence of the discrete phase might have taken place during compounding under certain processing conditions. In this study, we observed a transformation from a co-continuous to a dispersed morphology. Coalescence, which inevitably would take place before reaching a stable blend morphology, is a physical phenomenon which is associated with a kinetic process [23–25]. Breakup of the discrete phase may also take place in the pressure-driven flow of dispersed two-phase fluids [26]. To the best of our knowledge, theoretical treatment of breakup and coalescence of the discrete phase during the processing of two-phase polymer blends has not been addressed in the literature, which requires greater attention in the future.

References

[1] Han CD, Yu TC. Polym Engng Sci 1972;12:81.
[2] Han CD, Kim YW. Trans Soc Rheol 1975;19:245.
[3] Han CD. Rheology in polymer processing. New York: Academic Press, 1976 chapter 7.
[4] Han CD. Multiphase flow in polymer processing. New York: Academic Press, 1981 chapter 4.
[5] Nelson CJ, Avgeropoulos GN, Weisser FC, Böhm GGA. Angew Makromol Chem 1977;60/61:49.
[6] Van Oene H. In: Paul DR, Newman S, editors. Polymer blends, 1. New York: Academic Press, 1978. p. 295.
[7] Miles IS, Zurek A. Polym Engng Sci 1988;28:796.
[8] Ho RM, Wu CH, Su AC. Polym Engng Sci 1990;30:511.
[9] Favis BD, Therrien D. Polymer 1991;32:1474.
[10] He J, Bu W, Zeng J. Polymer 1997;38:6347.
[11] Shih C-K. Polym Engng Sci 1995;35:1688.
[12] Sundararaj U, Macosko CW, Shi C-K. Polym Engng Sci 1996;36:1769.
[13] Sundararaj U, Macosko CW, Rolando RJ, Chan HT. Polym Engng Sci 1992;32:1814.
[14] Scott CE, Macosko CW. Polymer 1995;36:461.
[15] Han CD, Lee KY, Wheeler NC. Polym Engng Sci 1996;36:1360.
[16] Lee JK, Han CD. Polymer 1999;40:2521.
[17] Van Oene H. J Colloid Interface Sci 1972;40:448.
[18] Han CD, Lem KW. Polym Engng Rev 1982;2:135.
[19] Han CD, Jhon MS. J Appl Polym Sci 1986;32:3809.
[20] Han CD. J Appl Polym Sci 1988;32:167.
[21] Han CD, Kim JK. Macromolecules 1989;22:4292.
[22] Cole KS, Cole RH. J Chem Phys 1941;9:341.
[23] Roland CM, Böhm GGA. J Polym Sci Polym Phys Ed 1984;22:79.
[24] Elmendorp JJ, Van der Vegt AK. Polym Engng Sci 1986;26:1332.
[25] Fortenly I, Zivny A. Polymer 1995;36:4113.
[26] Chin HB, Han CD. J Rheol 1980;24:1.